Expert Systems With Applications 305 (2026) 130935

Contents lists available at ScienceDirect

Expert Systems With Applications

journal homepage: www.elsevier.com/locate/eswa

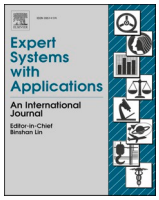

Availability assessment of demand-driven multi-state phased-mission system with performance sharing under reconfiguration mechanism

Gengshuo Hu [a], Xing Pan [a,b,*], Linchao Yang [c]

[a] School of Reliability and Systems Engineering, Beihang University, Beijing 100191, China
[b] National Key Laboratory of Reliability and Environmental Engineering, Beihang University, Beijing 100191, China
[c] Shool of Economics and Management, North China Electric Power University, Beinong Road, Changping, Beijing 102206, China

ARTICLE INFO

Keywords:
Multi-state phased-mission system
Common bus performance sharing
Demand-driven
Recovery mechanism
Universal generating function (UGF)

ABSTRACT

Multi-state phased-mission systems with common bus performance sharing (MS-PMSs-CBPS) are widely used in industries such as power supply and data processing systems. However, system availability modeling and assessment remain challenging due to the complexity of system structure and operation mechanisms. Additionally, existing studies have paid limited attention to the impact of demand variations on the number of operational components and the combined effects of disturbances and recovery mechanisms on system performance. To address these limitations, the paper first introduces a demand-driven MS-PMS-CBPS considering performance storage. In each mission phase, the number of operational components is determined by the probabilistic demand distribution, and performance surplus is stored for use in subsequent phase. Then, to enhance system availability under disturbances, the proposed model is extended by incorporating an adaptive backup reconfiguration (ABR) mechanism. Furthermore, we develop a Universal Generating Function (UGF)-based algorithm to evaluate the system instantaneous availability under ABR mechanism in the presence of random disturbances. Finally, we take a small power supply system as an example to verify the feasibility of the proposed methods.

1. Introduction

With the rapid advancement of industrial technologies, the complexity of industrial systems such as power supply systems (Zhao et al., 2018) and computing systems (Su et al., 2020) has significantly increased. These systems typically exhibit multiple characteristics, including multi-state, phased-mission, demand-driven, and common bus performance sharing. Specifically, they are composed of several subsystems with multi-state components. And they complete tasks in a series of continuous, non-overlapping mission phases. The number of operational components in each mission phase is determined by probabilistic demand. Additionally, the performance surplus can be reallocated to the subsystems with performance deficiency via the common bus. Although the incorporation of complex features enhances system functionality, it simultaneously increases susceptibility to random disturbances and complicates the modeling and assessment of system availability. Therefore, this paper aims to develop a modeling approach for a multi-state phased-mission system with common bus performance sharing, incorporating random disturbances and recovery mechanisms, to effectively capture the aforementioned characteristics for practical engineering applications.

Phased-mission systems (PMSs) are widely employed in fields such as aerospace (Yu et al., 2021) and power supply systems (Cheng et al., 2020). Existing studies on PMS reliability has primarily focused on structural modeling under various influencing factors, including imperfect failure coverage (IFC) (Xing, 2007), common cause failures (CCF) (Wang et al., 2015), external disturbances (Li et al., 2018), redundancy strategies (Levitin et al., 2020; Lin et al., 2023; Yu et al., 2021) and competitive failure (Tang et al., 2023). Moreover, PMS models incorporating multiple factors, including both internal and external disturbances (Peng et al., 2019), have also been developed. The structural configurations of PMSs are mainly classified into series–parallel system (Yu et al., 2021), k-out-of-n system (Chen et al., 2025) and linear-connected system (Levitin et al., 2014). However, most existing studies focus on components with binary states, which fail to accurately represent the potential states. The limitation stems from the binary-state modeling approach, which fails to account for component degradation and recovery process. Furthermore, the common bus

* Corresponding author at: School of Reliability and Systems Engineering, Beihang University, Beijing 100191, China.
E-mail address: panxing@buaa.edu.cn (X. Pan).

https://doi.org/10.1016/j.eswa.2025.130935
Received 10 August 2025; Received in revised form 16 December 2025; Accepted 18 December 2025
Available online 26 December 2025

performance sharing mechanism has been widely applied in industrial application due to its effectiveness in enhancing system reliability and availability through resource reallocation. Therefore, incorporating this mechanism into system modeling is essential.

Extensive research has been devoted to the reliability and availability modeling of multi-state systems with common bus performance sharing (MSSs-CBPS), and the system structures have been expanded from linear-connected (Levitin, 2011; Lisnianski & Ding, 2009) to series–parallel (Gu et al., 2026; Zhang et al., 2025), k-out-of-n (Wu et al., 2025; Zhao et al., 2024), linear sliding window (Xiao et al., 2020), tree-structured (Gu et al., 2025), star-structured (Azhdari & Ardakan, 2022; Su et al., 2021), network-structured (Azhdari et al., 2023; Huang et al., 2022), and ring-structured systems (Gu et al., 2025). Meanwhile, performance sharing mechanism can effectively enhance system reliability and availability by reallocating performance surplus to the components with performance deficiency. Therefore, many researchers have explored various bus structures, extending from single common bus (Gu, Wang, & Zhou, 2024b) to two performance sharing groups (Gu et al., 2024; Wu et al., 2021), multiple common buses (Gu, Wang, & Zhou, 2024a), and hierarchical performance sharing groups (Peng, 2019). With the growing interest in mission-driven applications, recent studies have also explored the modeling of multi-state phased-mission systems with common bus performance sharing (MS-PMSs-CBPS), incorporating external factors such as transmission loss and performance storage (Cheng et al., 2020), epistemic uncertainty (Cheng et al., 2021a), common cause failures (Cheng et al., 2021b; Yu et al., 2017), and weight of each component (Bhatt & Singh, 2025). However, these studies typically predefine a fixed number of operational components for each mission phase, which may not accurately reflect real-world system behavior. For example, the number of operational generators in a power supply system is determined by the probabilistic demand within the responsible area. Due to variability, it is impractical to assume a fixed number of operational components. Therefore, it is necessary to develop a demand-driven model that configures the number of operational components based on probabilistic demand.

Furthermore, random disturbances can significantly affect system performance. Therefore, it is necessary to investigate recovery mechanisms to mitigate the impact and ensure continuous system operation (Wang et al., 2025). Recent research on recovery mechanisms for MSS-CBPS has primarily focused on two categories: maintenance mechanisms (Levitin et al., 2019; Wu et al., 2024; Yi et al., 2019) and redundancy mechanisms (Peng et al., 2021; Sharifi & Taghipour, 2022). While maintenance mechanisms involve proactive actions, such as preventive and corrective maintenance to maintain system performance. Redundancy mechanisms typically provide backup resource that operate in parallel with primary components. However, these recovery mechanisms often overlook the interdependence among the components. Dynamic reconfiguration mechanisms are effective in addressing disturbances by reallocating resources to maintain system operation (Alhozaimy et al., 2024; Hu et al., 2025). Despite their critical role in real-world engineering applications, these aspects remain insufficiently explored in existing research.

Availability is a critical metric for evaluating systems under recovery mechanisms and random disturbances, as it reflects their capability to maintain functionality over time (Rudek & Rudek, 2024). The integration of the Markov process with the Universal Generating Function (UGF) has been widely adopted for system availability assessment. The Markov process is widely used to model state transitions of multi-state components (Wu et al., 2024). Meanwhile, UGF has been widely used in the availability assessment of multi-state systems due to its efficiency and analytical simplicity (Levitin, 2005). Due to the diverse structures and operational mechanisms of various systems, existing studies often require customized UGF algorithms for availability evaluation. The integration of demand-driven configurations and recovery mechanisms significantly increases the complexity of availability assessment. Meanwhile, instantaneous availability effectively captures real-time variation during each mission phase. Therefore, it is necessary to develop an adaptable UGF algorithm capable of evaluating system instantaneous availability under demand-driven configuration and recovery mechanisms.

Although existing studies have significantly advanced the modeling and assessment of MS-PMSs-CBPS, several important issues need to be addressed. First, although existing studies have extensively examined the impact of random disturbances on component states, they have overlooked the demand variability within mission phases. Overlooking this variability may result in inaccurate system availability evaluations. Therefore, it is critical to develop a demand-driven modeling approach that accurately reflects probabilistic demand variations during each mission phase. Second, while recovery mechanisms under random disturbances have been studied for MSSs-CBPS, their application in MS-PMSs-CBPS remains limited. Moreover, existing recovery mechanisms primarily address isolated failures and often overlook system-level interdependencies, which limits their effectiveness in responding to random disturbances. In particular, MS-PMSs-CBPS are inherently more susceptible to disruptions due to task dependence and complex operating mechanisms. Therefore, it is meaningful to study system-level recovery mechanisms for MS-PMSs-CBPS under random disturbances. Finally, most researchers have concentrated on long-term availability. However, in PMSs, obtaining instantaneous availability in each mission phase is essential, as it reflects real-time variations during mission transitions. Therefore, it is essential to develop UGF-based algorithms to evaluate system instantaneous availability under recovery mechanisms.

To address these gaps, the contributions are as follows: First, we extend the existing MS-PMS-CBPS considering performance storage model by incorporating probabilistic demand, which determines the number of operational components during each mission phase. Second, we propose an adaptive backup reconfiguration (ABR) mechanism to enhance system availability under random disturbances. Third, we develop a UGF-based algorithm for the evaluation of system instantaneous availability under the recovery mechanism. Finally, we take a small-scale power supply system as an example to analyze the trend of instantaneous availability under the recovery mechanism.

The proposed modeling and assessment methods are inspired by practical engineering applications. For example, in small-scale power supply systems, the number of operational generators in each power plant is adjusted according to the varying electricity demand. Power plants with electricity surplus can transmit excess electricity to other plants with electricity deficiency through the transmission bus. Additionally, when operational generators are affected by random disturbances such as degradation or strikes, standby generators are activated sequentially to maintain continuous power supply. Similar mechanisms can also be observed in distributed computing systems, where the number of active computing nodes is adjusted according to task demand, surplus computational resource is shared among nodes, and standby nodes are activated sequentially under random disturbances to maintain system continuity.

The structure of this paper is organized as follows: Section 2 introduces a novel structure of a demand-driven MS-PMS-CBPS. Moreover, the influence of random disturbances and recovery mechanisms is also introduced. Section 3 provides the UGF-based instantaneous availability assessment algorithms suitable for the system with recovery mechanisms. Section 4 takes a small-scale power supply system as an example. Section 5 shows the conclusion and future work.

2. Model description

2.1. System structure

(1) MS-PMS-CBPS

The MS-PMS-CBPS consists of n subsystems and a performance storage (PS) device, connected via a common bus (Fig. 1) (Cheng et al., 2020). It is designed to accomplish H independent mission phases.

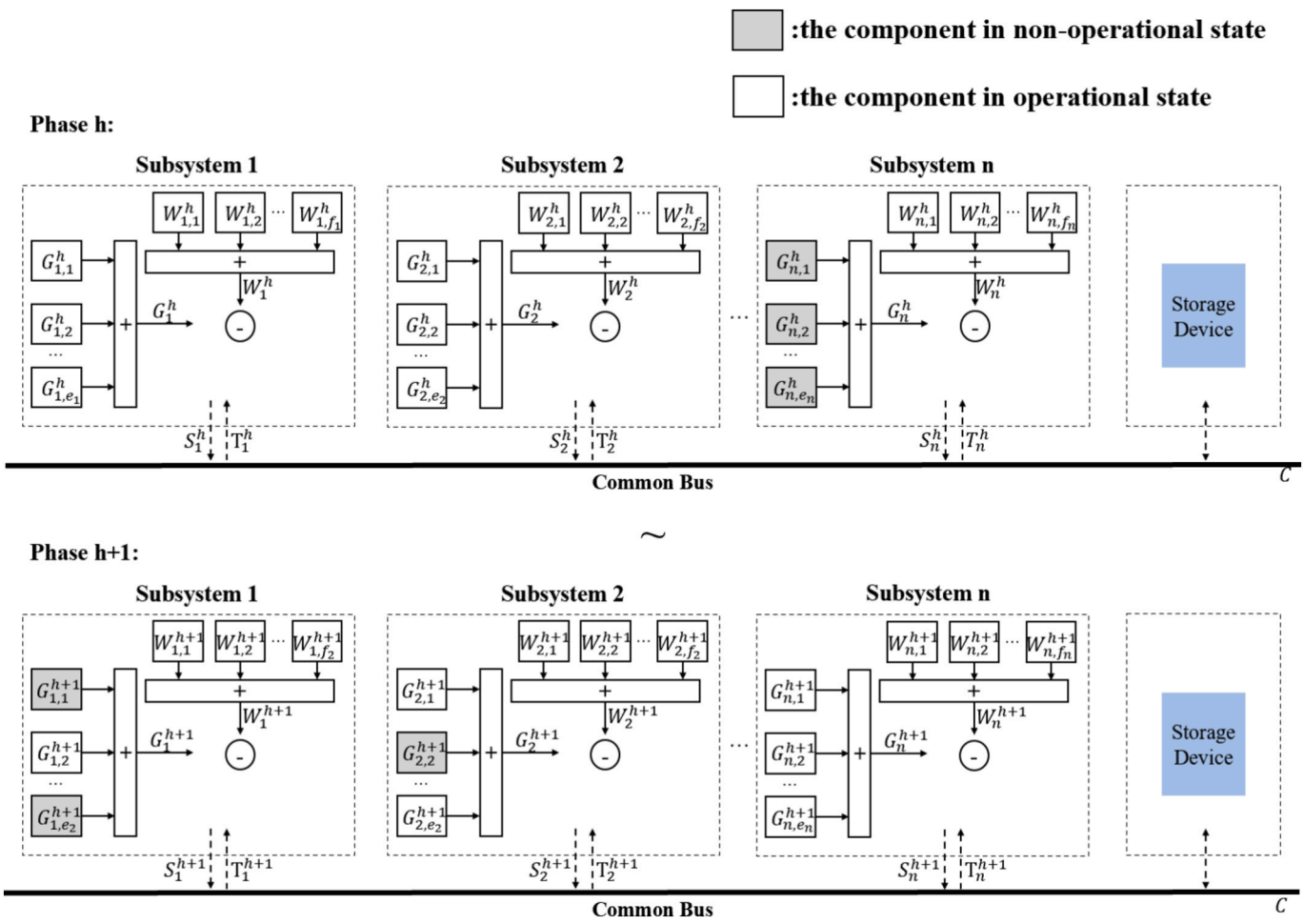

Fig. 1. The structure of MS-PMS-CBPS-PS.

Subsystem i comprises e_i identical multi-state components. The total performance G_i^h of components in subsystem i need to satisfy the total demand W_i^h in subsystem i during mission phase h. Meanwhile, the performance surplus S_i^h can be transmitted to the subsystems with performance deficiency through the common bus, which has a maximum transmission capacity C. The reallocated performance surplus T_i^h is randomly distributed among the subsystems with performance deficiency. After performance sharing, if any subsystem still experiences performance deficiency, the system is considered failed. Conversely, any remaining performance surplus is collected by the storage device with a capacity of $C_{storage}$ and efficiency η_s, and used in the next mission phase. Moreover, the sets of operational subsystems vary across different mission phases due to changing operational requirements. Nevertheless, the internal structure of each subsystem remains consistent throughout all phases.

However, in practical engineering applications, the number of components within each subsystem is determined based on the probabilistic demand in each mission phase. Specifically, each demand levels correspond to a specific number of operational components, with associated probabilities. In addition, the system may be subject to both internal disturbances (e.g., component degradation) and external disturbances (e.g., natural disasters). Implementing appropriate recovery mechanisms is essential to enhance system availability under disturbances. Therefore, it is critical to incorporate these factors into system modeling and availability assessment.

(2) Demand-driven MS-PMS-CBPS.

We extend the existing model by incorporating the demand-driven characteristic, as illustrated in Fig. 2. Unlike the existing model that predefine a fixed number of operational components for each mission phase (Cheng et al., 2020), the proposed model configures the number of operational components based on the probabilistic demand distribution within each phase, thereby avoiding unnecessary over-provisioning and improving the accuracy of availability assessment. Moreover, if a subsystem experiences performance deficiency, other subsystems and the storage device with performance surplus reallocate the allocable performance to it via the common bus. When there is no performance deficiency in any subsystems, the system remains in the operation state.

2.2. System mechanism

Random disturbances, component-level recovery, and system-level recovery mechanisms affect the operation state of the system. Therefore, they need to be considered in the extended model, shown in Fig. 3.

(1) Random disturbances

During the operation, external disturbances affecting components are categorized into three types: invalid, normal, and extreme. The probability of an invalid disturbance affecting component j in subsystem i is denoted by $q_{i,0}$. This type of disturbance has no impact on the component. The normal disturbance, with probability $q_{i,1}$, causes the component to transition to a worse state. The extreme disturbance, occurring with probability $q_{i,2}$, causes the component to transition from the working state to the fault state. Additionally, the occurrence of disturbances affecting component j can be modeled as a homogenous Poisson process with an arrival rate $\lambda_{i,j}$ (Tan et al., 2023). This assumption reflects the independence of disturbances and assumes a uniform distribution of their occurrence times over the specified time

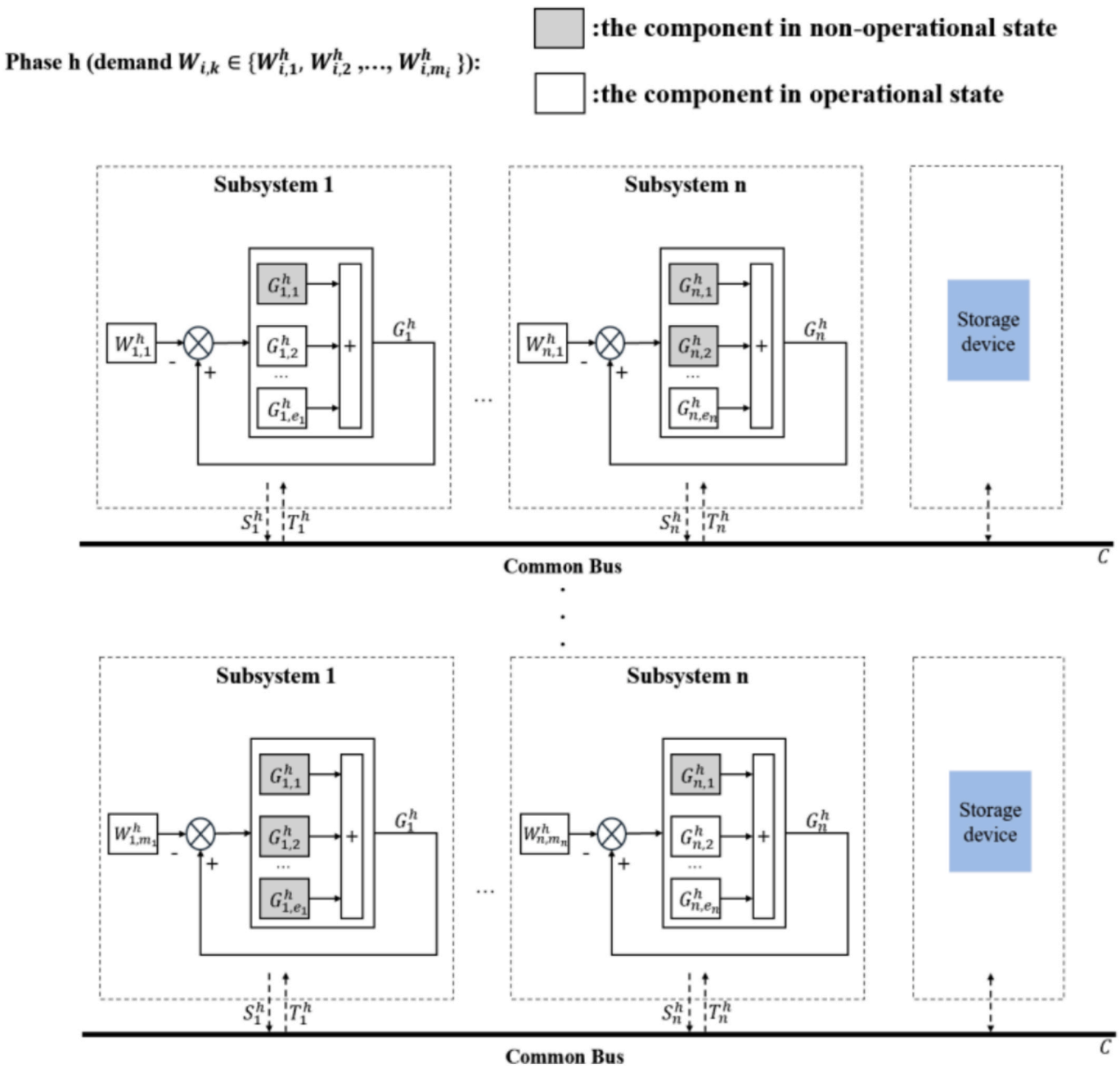

Fig. 2. Demand-driven MS-PMS-CBPS-PS at phase h.

horizon. Furthermore, internal disturbances (degradation) also affect the components over time. The degradation time follows an exponential distribution with the degradation rate $\bar{\lambda}_{i,j}$ (Wu et al., 2024).

(2) Component-level recovery mechanism

When a component enters the failed state, it can be restored to the normal working state through special maintenance, whose repair time is modeled by an exponential distribution with rate $\theta_{i,j}$. In contrast, corrective maintenance restores the component to its previous degraded state rather than fully recovering it to full functionality, and its repair time follows an exponential distribution with rate of $\mu_{i,j}$.

(3) System-level recovery mechanism

Preventive maintenance is a proactive maintenance mechanism widely used in engineering, where system components are serviced at regular intervals based on a fixed schedule to prevent failures caused by random disturbances (Wu et al., 2024). However, existing studies do not adequately consider the characteristics of PMSs, where mission phases are interdependent and maintenance actions in one phase can influence the availability of subsequent phases. To address this issue, rotational maintenance (RM), a form of preventive maintenance, can be implemented to ensure continuous operation by periodically servicing components. It involves cyclically alternating the components within a subsystem based on a predefined cycle T_i. Specifically, once the rotation cycle T_i is completed, the idle components are activated to the operational state, and the previously operational components undergo preventive maintenance. The maintenance duration is τ_i, and the components are assumed to be fully restored to a condition as good as new after preventive maintenance.

In contrast to the fixed-cycle nature of the RM mechanism, the ABR mechanism is introduced as a passive mechanism that responds to disturbances by reallocating resources to maintain system operation. Specially, when a subsystem experiences a performance deficiency, it activates the idle backup components sequentially and reallocates the

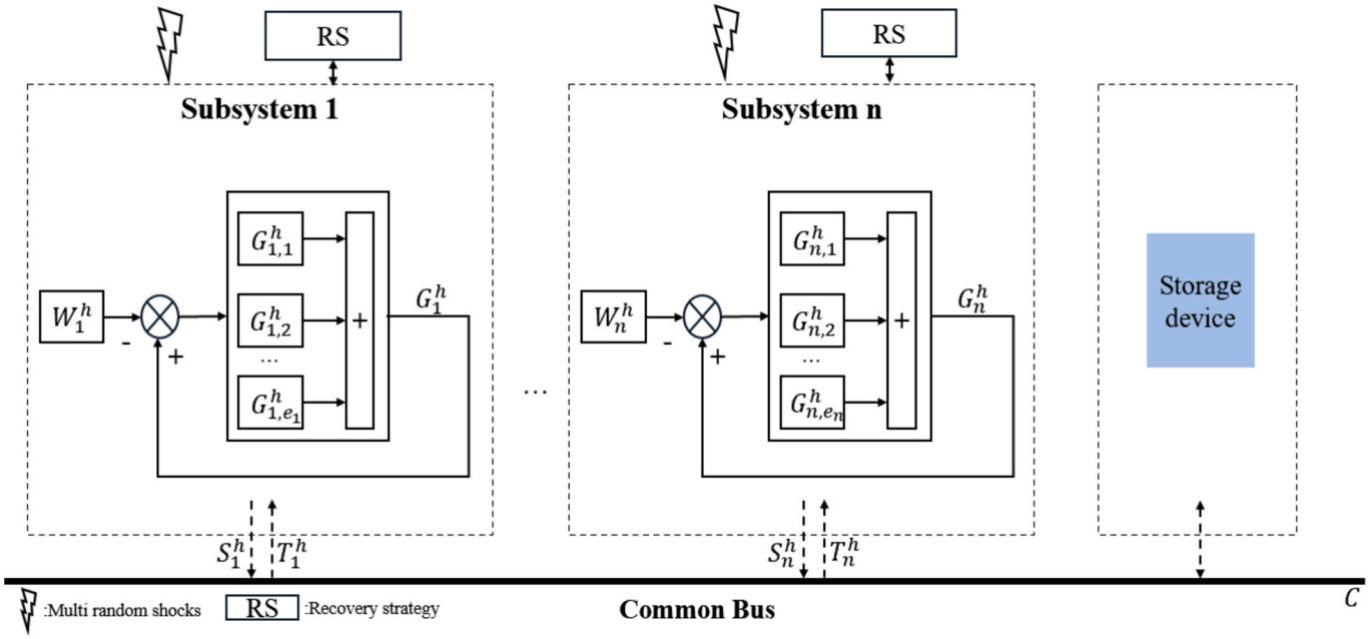

Fig. 3. Proposed extend model considering random disturbances and recovery strategies.

tasks accordingly. After each activation, if there is still performance deficiency in the subsystem, the next available backup component is activated. If the performance remains unable to meet the demand after all its backups are utilized, a portion of the tasks is further reallocated to operational components in other subsystem via the common bus, thereby ensuring continuous system operation.

The examples of these recovery mechanisms are presented in Appendix A1.

2.3. System mathematic description

This study investigates repairable multi-state components, which are subject to random disturbances and operate under component-level recovery mechanisms. Since the state transitions of each component depend solely on its current state, the behavior of each component can be modeled as a continuous-time Markov process, where the variable t is continuous and represents the temporal evolution of component performance.

$$P(X_{t+1} = x_{t+1} | X_t = x_t, X_{t-1} = x_{t-1}, \ldots, X_0 = x_0) = P(X_{t+1} = x_{t+1} | X_t = x_t) \tag{1}$$

Where X_t indicates the state of the component at time t, and X_{t+1} is the future state.

The transition rate is determined by the degradation, external disturbances, and recovery processes. Therefore, the state transition rate matrix can be derived as:

$$Q_{i,j} = Q_{i,j,in} + Q_E + Q_{i,j,r} \tag{2}$$

Where $Q_{i,j,in}$ denotes the intrinsic degradation matrix, determined by the degradation rate of the component $\overline{\lambda}_{i,j,m_{i,j},n_{i,j}}$; Q_E denotes the external disturbances matrix which represents the effect of random disturbances. It is calculated based on the arrive rate $\lambda_{i,j}$ of random disturbances and their probability of occurrence $(q_{i,0}, q_{i,1}, q_{i,2})$; $Q_{i,j,r}$ denotes the compo-

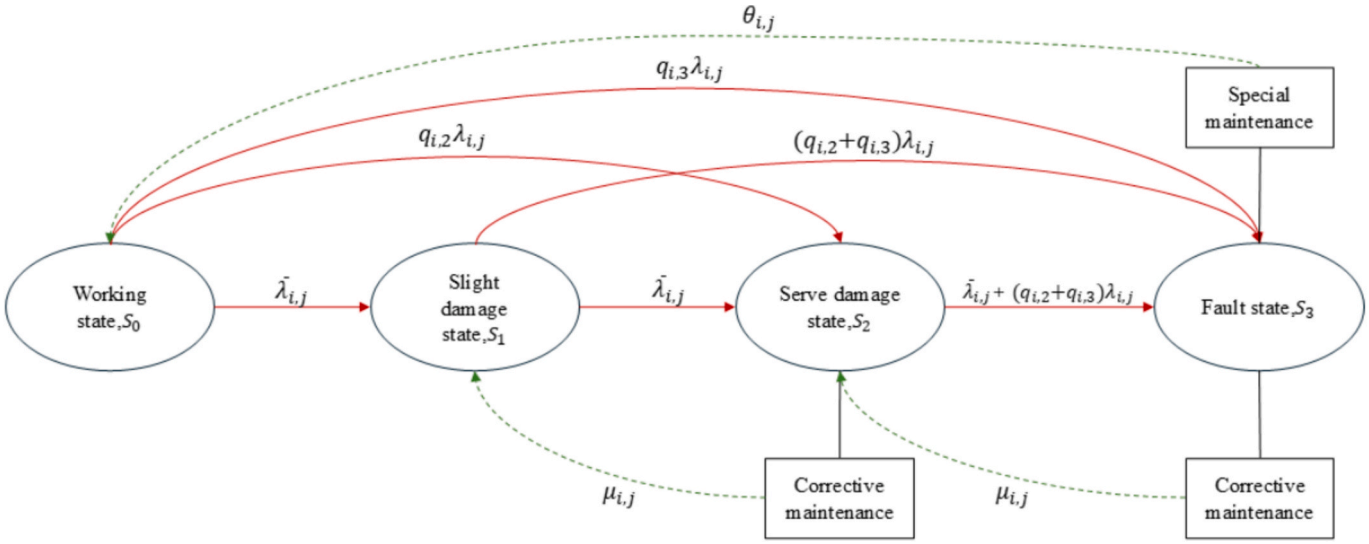

Fig. 4. The illustrated example of the Markov process of a component.

nent recovery matrix, determined by the repair rates of corrective maintenance $\mu_{i,j}$ and special maintenance $\theta_{i,j}$. An illustrated example is provided in Fig. 4 for better clarity.

The state transition matrix in the example can be represented as

$$Q_{ij}=\begin{bmatrix} -\left(\overline{\lambda}_{i,j}+q_{i,2}\lambda_{i,j}+q_{i,3}\lambda_{i,j}\right) & \overline{\lambda}_{i,j} & q_{i,2}\lambda_{i,j} & q_{i,3}\lambda_{i,j} \\ 0 & -\left(\overline{\lambda}_{i,j}+\left(q_{i,2}+q_{i,3}\right)\lambda_{i,j}\right) & \overline{\lambda}_{i,j} & \left(q_{i,2}+q_{i,3}\right)\lambda_{i,j} \\ 0 & \mu_{i,j} & -\left(\mu_{i,j}+\overline{\lambda}_{i,j}+\left(q_{i,2}+q_{i,3}\right)\lambda_{i,j}\right) & \overline{\lambda}_{i,j}+\left(q_{i,2}+q_{i,3}\right)\lambda_{i,j} \\ \theta_{i,j} & 0 & \mu_{i,j} & -\left(\theta_{i,j}+\mu_{i,j}\right) \end{bmatrix} \tag{3}$$

The Kolmogorov function can be used to calculate the state probabilities $P_{i,j}(t)$ of the component j.

$$\frac{d}{dt}P_{i,j}(t)=P_{i,j}(t)Q_{i,j} \tag{4}$$

According to Eq. (4), the set of state probabilities of component performance levels can be derived, $\left[\alpha_{i,j,1},\alpha_{i,j,2},\cdots,\alpha_{i,j,M_{i,j}}\right]$. Notably, the state probabilities vary over time, and $\alpha_{i,j,1}$ represents the probability that the component is in its normal working state.

During normal operation, the minimum number of active components in the initial configuration is determined by the subsystem probabilistic demand and maximum performance of its components, as given in Eq. (5).

$$n_i^h=\lceil\frac{W_i^h}{G_{i,j,\max}^h}\rceil \tag{5}$$

Where W_i^h represents the probabilistic demand of subsystem i in mission phase h. It can take multiple discrete values, each associated with a certain probability, and remains constant once a demand level is realized within the phase. $G_{i,j,\max}^h$ denotes the performance of component j in its normal working state within the subsystem i. $\lceil\ \rceil$ represents the celling function, which rounds a given value up to the nearest integer. Additionally, this represents the initial configuration without considering uncertainty, while system-level recovery mechanisms later address random disturbances to satisfy the demand.

During mission phase h, the performance of subsystem i can be denoted as

$$G_i^h(t)=\sum_{j=1}^{n_i^h}G_{i,j}^h(t) \tag{6}$$

Where $G_{i,j}^h(t)$ is the performance of component i in subsystem j and it varies continuously over time due to random disturbances and recovery mechanisms.

Based on the performance $G_i^h(t)$ and demand W_i^h of subsystem i, the performance surplus $S_i^h(t)$ and performance deficiency $D_i^h(t)$ at time t during mission phase h can be represented as

$$S_i^h(t)=\max\left(G_i^h(t)-W_i^h,0\right) \tag{7}$$

$$D_i^h(t)=\max\left(W_i^h-G_i^h(t),0\right) \tag{8}$$

The total performance surplus $S^h(t)$ and total performance deficiency $D^h(t)$ at time t can be represented as

$$S^h(t)=\sum_{i=1}^{n}S_i^h(t) \tag{9}$$

$$D^h(t)=\sum_{i=1}^{n}D_i^h(t) \tag{10}$$

When there are existing subsystems with performance deficiency, the performance surplus $S^h(t)$ and the performance stored in the storage device during the previous mission phase $V^{h-1}(t)$ can be reallocated by the common bus with capacity $C(t)$. The reallocated performance $T(t)$ can be formulated as

$$T^h(t)=\min\left(S^h(t)+V^{h-1}(t),C(t)\right) \tag{11}$$

Meanwhile, the redistributed performance is allocated to subsystems with performance deficiency randomly. Additionally, if there is remaining performance surplus after performance sharing, it can be stored in the storage device. After performance sharing, the performance surplus $\overline{S}^h(t)$, performance deficiency $\overline{D}^h(t)$, and stored performance $\overline{C}_{storage}^h(t)$ of the system can be calculated by Table 1.

The system instantaneous availability $A_0^h(t)$ is evaluated as the probability that no performance deficiency exists in the system after performance sharing at time t during mission phase h, which also serves as the criterion for determining the successful completion of the mission phase.

$$A_0^h(t)=Pr\left(\overline{D}^h(t)=0\right) \tag{12}$$

The system-level recovery mechanisms are adopted to sustain its operation under disturbances. Under the RM mechanism, components first operate for a fixed cycle T, after which they undergo preventive maintenance. During this maintenance, the components are fully restored to their normal working state. The duration of the maintenance is denoted as T_r. Therefore, at time t, the probability that the component j in the subsystem i in working state is represented as

$$P_{i,j}\left(G_{i,j}^h(t)=G_{i,j,\max}^h\right)=\begin{cases}\alpha_{i,j,1}(\ mod\ (t,T+T_r)) & 0\leqslant mod\ (t,T+T_r)<T\\ 0 & T\leqslant mod\ (t,T+T_r)<T+T\end{cases} \tag{13}$$

Where $\alpha_{i,j,1}(\ mod\ (t,T+T_r))$ is the probability that the component j is in its normal working state.

Since the system structure and operation mechanisms remain constant over time, only the component state probabilities vary due to maintenance cycle. Table 1 can be applied to evaluate instantaneous availability.

For the ABR mechanism, when a subsystem experiences a performance deficiency, its backup components are activated sequentially in response. After each activation, a portion of the subsystem's workload is reallocated to the newly activated backup components to satisfy the performance deficiency and restore subsystem functionality. If the performance deficiency persists after all available backups have been activated, the remaining workload is further redistributed to operational components in other subsystems through the common bus, ensuring the continuity of overall system operation. Under ABR mechanism, the performance surplus $\widetilde{S}^h(t)$, performance deficiency $\widetilde{D}^h(t)$, and stored performance $\widetilde{C}_{storage}^h(t)$ can be obtained by Table 2.

Table 1
Algorithm of performance sharing.

Input: Total performance surplus $S^h(t)$; total performance deficiency $D^h(t)$; reallocated performance $T^h(t)$; performance storage $V^{h-1}(t)$; storage efficiency η_s, and storage capacity $C_{storage}$.

Output: Performance deficiency $\overline{D}^h(t)$, performance surplus $\overline{S}^h(t)$, and stored performance $\overline{C}^h_{storage}(t)$.

1: The performance deficiency is $\overline{D}^h(t) = \max(D^h(t) - T^h(t), 0)$;
2: The available stored performance is $AP^h(t) = \max(T^h(t) - S^h(t), 0)$;
3: The consumed stored performance is $UP^h(t) = \min(AP^h(t), \max(D^h(t) - S^h(t), 0))$
4: The remaining stored performance is $\overline{RP}^h(t) = \max(V^{h-1}(t) - UP^h(t), 0)$;
5: The updated stored performance is $\overline{C}^h_{storage}(t) = \min(\overline{RP}^h(t) + \eta_s \times \max(S^h(t) - D^h(t), 0), C_{storage})$;
6: The performance surplus is $\overline{S}^h(t) = \max\left(S^h(t) + V^{h-1}(t) - D^h(t) - \overline{C}^h_{storage}(t), 0\right)$;
7: **Return** $\overline{D}^h(t)$, $\overline{S}^h(t)$, and $\overline{C}^h_{storage}(t)$.

The instantaneous availability under the ABR mechanism $A^h(t)$ at time t during mission phase h can be calculated as

$$A^h(t) = Pr\left(\widetilde{D}^h(t) = 0\right) \tag{14}$$

3. The algorithm of system availability evaluation

3.1. System instantaneous availability evaluation by UGF

Compared with other methods, such as Monte Carlo simulation, the UGF method demonstrates notable advantages regarding computational efficiency and result accuracy (Tian et al., 2023). Specifically, the UGF method adopts a concise and intuitive process to represent system performance and demand states and calculate the corresponding probability distributions.

During mission phase h, the demand $W_i^h(t)$ of the subsystem i is randomly obtained from vector $\left[w^h_{i,1}, w^h_{i,2}, \ldots w^h_{i,P_i}\right]$, and the probability mass function (pmf) of demand in UGF form is

$$\omega_i^h(z) = \sum_{p_i=1}^{P_i} \beta_{i,p_i} z^{w^h_{i,p_i}} \tag{15}$$

Where β_{i,p_i} is the probability that the demand of subsystem i is w^h_{i,p_i} during mission phase h,$p_i = 1, 2, \ldots, P_i$.

The performance $G^h_{i,j}(t)$ of the component j in the subsystem i is randomly obtained from vector $\left[g^h_{i,j,1}, g^h_{i,j,2}, \ldots, g^h_{i,j,M_{i,j}}\right]$, and $g^h_{i,j,1}$ is the performance of component j in working state. The pmf of performance in UGF form is

$$u^h_{i,j}(z) = \sum_{m_{i,j}=1}^{M_{i,j}} \alpha_{i,j,m_{i,j}} z^{g^h_{i,j,m_{i,j}}} \tag{16}$$

Where $\alpha_{i,j,m_{i,j}}$ is the probability that the performance of component j is $g^h_{i,j,m_{i,j}}$ during mission phase h, and it is calculated by Eq. (4),$m_{i,j} = 1,2,\ldots, M_{i,j}$.

Based on Eq. (5) and (6), the pmf of performance $G_i^h(t)$ of subsystem i in UGF form can be obtained when the demand w^h_{i,p_i} is given.

Table 2
Algorithm of the adaptive backup reconfiguration mechanism.

Input: Performance surplus of each subsystem $S_i^h(t), i = 1, 2, \cdots, n$;
performance deficiency of each subsystem $D_i^h(t), i = 1, 2, \cdots, n$;
the number of backup component in each subsystem $n_{b_i}, i = 1, 2, \cdots, n$;
performance of backup component in each subsystem $S_{b_{i,j}}(t), i = 1, 2, \cdots, n, j = 1, 2, \cdots, n_{b_i}$;
transmission capacity $C(t)$; performance storage $V^{h-1}(t)$;
storage efficiency η_s; and storage capacity $C_{storage}$.

Output: Performance surplus $\widetilde{S}^h(t)$, performance deficiency $\widetilde{D}^h(t)$, and stored performance $\widetilde{C}^h_{storage}(t)$.

1: **for** $i = 1 : n$
2: **if** $S_i^h(t) - D_i^h(t) < 0$
3: set $\widehat{S}_i = S_i^h(t)$;
4: **for** $j = 1 : n_{b_i}$
5: $\widehat{S}_i = \widehat{S}_i + S_{b_{i,j}}(t)$;
6: **if** $\widehat{S}_i \geq D_i^h(t)$;
7: **break**
8: **end for**
9: **else**
10: $\widehat{S}_i = S_i^h(t)$;
11: **end if**
12: **end for**
13: **for** $i = 1 : n$
14: $\widehat{S}_i^h(t) = \max(\widehat{S}_i - D_i^h(t), 0)$;
15: $\widehat{D}_i^h(t) = \max(D_i^h(t) - \widehat{S}_i, 0)$;
16: **end for**
17: The reallocated performance is $\widehat{T}^h(t) = \min(\sum_{i=1}^n \widehat{S}_i^h(t) + V^{h-1}(t), C(t))$;
18: The performance deficiency under ABR mechanism is $\widetilde{D}^h(t) = \max(\sum_{i=1}^n \widehat{D}_i^h(t) - \widehat{T}^h(t), 0)$;
19: The available performance storage is $\widetilde{AP}^h(t) = \max(\widehat{T}^h(t) - \sum_{i=1}^n \widehat{S}_i^h(t), 0)$;
20: The consumed performance storage is $\widetilde{UP}^h(t) = \min\left(\widetilde{AP}^h(t), \max(\sum_{i=1}^n \widehat{D}_i^h(t) - \sum_{i=1}^n \widehat{S}_i^h(t), 0)\right)$;
21: The remaining performance storage is $\widetilde{RP}^h(t) = \max\left(V^{h-1}(t) - \widetilde{UP}^h(t), 0\right)$;
22: The updated stored performance is $\widetilde{C}^h_{storage}(t) = \min\left(\widetilde{RP}^h(t) + \eta_s \times \max(\sum_{i=1}^n \widehat{S}_i^h(t) - \sum_{i=1}^n \widehat{D}_i^h(t), 0), C_{storage}\right)$;
23: The performance surplus is $\widetilde{S}^h(t) = \max\left(\sum_{i=1}^n \widehat{S}_i^h(t) + V^{h-1}(t) - \sum_{i=1}^n \widehat{D}_i^h(t) - \widetilde{C}^h_{storage}(t), 0\right)$;
24: **Return** $\widetilde{S}^h(t)$, $\widetilde{D}^h(t)$, and $\widetilde{C}^h_{storage}(t)$.

$$u_{i,p_i}^h(z) = u_{i,1}^h(z) \oplus \ldots \oplus u_{i,n_{i,p_i}}^h(z) \tag{17}$$

$$= \sum_{m_{i,1}=1}^{M_{i,1}} \cdots \sum_{m_{i,n_{p_i}}=1}^{M_{i,n_{p_i}}} \left(\prod_{k=1}^{n_{p_i}} \alpha_{i,k,m_k}\right) z^{\sum_{k=1}^{n_{p_i}} g_{i,k,m_k}^h}$$

$$= \sum_{r=1}^{M_i} \alpha_{i,p_i,r} z^{g_{i,p_i,r}^h}$$

Where M_i is the number of terms in UGF after collecting like term, $g_{i,p_i,r}^h$ represents the total performance of subsystem i, $\alpha_{i,p_i,r}$ is the joint probability that the total performance of subsystem i is $g_{i,p_i,r}$. n_{i,p_i} is the number of the components in the operational state.

$$n_{i,p_i} = \lceil \frac{w_{i,p_i}^h}{g_{i,j,1}^h} \rceil \tag{18}$$

Based on Eq. (7) and (8), the combination operator $\otimes$ is used to obtain the joint pmf of the performance surplus $S_i^h(t)$ and deficiency $D_i^h(t)$ of subsystem i in UGF form, given a demand w_{i,p_i}^h.

$$\Delta_{i,p_i}^h(z) = \beta_{i,p_i} z^{w_{i,p_i}^h} \otimes u_{i,p_i}^h(z) \tag{19}$$

$$= \sum_{r=1}^{M_i} \alpha_{i,p_i,r} \beta_{i,p_i} z^{\max\left(g_{i,p_i,r}^h - w_{i,p_i}^h, 0\right), \max\left(w_{i,p_i}^h - g_{i,p_i,r}^h, 0\right)}$$

According to the performance surplus and deficiency of subsystem i in UGF form under different demands $\Delta_{i,p_i}^h(z)$, we calculate the joint pmf of the performance surplus and deficiency of subsystem i in UGF form under different demand $\Delta_i^h(z)$ during mission phase h through summation.

$$\Delta_i^h(z) = \sum_{p_i=1}^{P_i} \Delta_{i,p_i}^h(z) \tag{20}$$

$$= \sum_{b=1}^{B^h} \pi_b z^{s_b^h, d_b^h}$$

Where B^h is the number of terms in UGF after collecting like term, π_b is joint probability that the system performance surplus is s_b^h and the system performance deficiency is d_b^h during mission phase h.

The transmission capacity of the common bus is randomly obtained from vector $[c_1, c_2, \ldots, c_L]$, the pmf of transmission capacity in UGF is

$$\eta(z) = \sum_{l=1}^{L} \delta_l z^{c_l} \tag{22}$$

Where, δ_l is the probability that the capacity of the common bus is c_l,$l = 1, 2, \ldots, L$.

In the mission phase h, if no performance surplus has been stored in the storage device during the previous phase, the pmf of performance storage in UGF is

$$U_C^h(z) = \sum_{b=1}^{B^h} \sum_{l=1}^{L} \pi_b \delta_l z^{\min\left(\eta_s \max\left(\min\left(s_b^h, c_l\right) - d_b^h, 0\right), C_s\right)} \tag{23}$$

$$= \sum_{b_1=1}^{B_1^h} \sigma_{b_1}^h z^{st_{b_1}^h}$$

Where C_s is the maximum storage capacity,η_s is the storage efficiency. B_1^h is the number of terms in UGF after collecting like term,$\sigma_{b_1}^h$ is the probability that the performance storage is $st_{b_1}^h$.

According to Eqs. (21)-(23), Table 1 is used to obtain the joint UGF of total performance surplus, total performance deficiency, and performance storage during mission phase h.

$$\overline{U}_\Omega^h(z) = U_\Omega^h(z) \otimes_{\leftrightarrow} U_C(z) \otimes_{\leftrightarrow} \eta(z) \tag{24}$$

$$= \sum_{b=1}^{B^h} \sum_{l=1}^{L} \sum_{b_1=1}^{B_1^h} \pi_b \delta_l \sigma_{b_1}^h z^{\max\left(s_b^h - d_b^h - \min\left(\eta_s \max\left(\min\left(s_b^h, c_l\right) - d_b^h, 0\right), C_s\right), 0\right), \max\left(d_b^h - \min\left(s_b^h, c_l\right), 0\right), \min\left(\eta_s \max\left(\min\left(s_b^h, c_l\right) - d_b^h, 0\right), C_s\right)}$$

$$= \sum_{p_i=1}^{P_i} \sum_{r=1}^{M_i} \alpha_{i,p_i,r} \beta_{i,p_i} z^{\max\left(g_{i,p_i,r}^h - w_{i,p}^h, 0\right), \max\left(w_{i,p}^h - g_{i,p_i,r}^h, 0\right)}$$

$$= \sum_{v_i=1}^{V_i} \gamma_{i,v_i} z^{s_{i,v_i}^h, d_{i,v_i}^h}$$

Where V_i is the number of terms in UGF after collecting like term, γ_{i,v_i} is the joint probability that the performance surplus is s_{i,v_i}^h and performance deficiency is d_{i,v_i}^h during mission phase h.

The combination operator $\oplus$ is used to obtain the joint pmf of total performance surplus $S^h(t)$ and total performance deficiency $D^h(t)$ of system in UGF form through iterative calculation.

$$U_\Omega^h(z) = \Delta_1^h(z) \oplus \Delta_2^h(z) \oplus \ldots \oplus \Delta_n^h(z) \tag{21}$$

$$= \sum_{v_1=1}^{V_1} \cdots \sum_{v_n=1}^{V_n} \left(\prod_{i=1}^{n} \gamma_{i,v_i}\right) z^{\sum_{i=1}^{n} s_{i,v_i}^h, \sum_{i=1}^{n} d_{i,v_i}^h}$$

$$= \sum_{j_a=1}^{J_A} pr_{j_a} z^{\overline{s}_{j_a}^h, \overline{d}_{j_a}^h, \overline{U}_{j_a}^h}$$

Where J_A is the number of terms in UGF after collecting like term,pr_{j_a} is the joint probability that the total performance surplus is $\overline{s}_{j_a}^h$, the total performance deficiency is $\overline{d}_{j_a}^h$, and the performance storage is $\overline{U}_{j_a}^h$.

According to Eq. (12) and Eq. (24), during phased mission h, the system instantaneous availability $A_0^h(t)$ after performance sharing is calculated by

$$A_0^h(t) = Pr\left(\overline{d}_{j_a}^h = 0\right) \tag{25}$$

Additionally, based on Eq. (24), Eq. (25) and Table 1, the instantaneous availability in the subsequent mission phases can be calculated using a similar approach.

Under the RM mechanism, components operate in a fixed cycle and are fully restored after maintenance. As the mission schedule is predefined and the system structure remains unchanged across mission

phases, only the component state probabilities evolve over time. Consequently, Eqs. (15)-(25) and Table 1 can be applied to evaluate the system instantaneous availability based on time-dependent probabilities.

3.2. System instantaneous availability evaluation under ABR mechanism

For the ABR mechanism, unlike traditional redundancy mechanism that maintain fixed standby components independent of actual performance deficiency (Su et al., 2020), the proposed mechanism represents a dynamic extension of demand-driven modeling. Backup components are sequentially activated only when performance deficiency arises, and tasks are reallocated to sustain subsystem functionality. The ABR mechanism introduces significant modeling complexity due to the combinatorial expansion of component activation scenarios, posing a major challenge for accurate availability evaluation. To address this issue, we propose a UGF-based Cutting and Adaptive Backup Reconfiguration (UCAR) algorithm based on Table 2, which mitigates the state space explosion by pruning the performance states that already meet the demand and dynamically activating backup components only when deficiencies occur. It is provided in Fig. 5.

First, the UGF of performance surplus and deficiency of subsystem i, $\Delta_i^h(z)$ is calculated based on Eqs. (15)-(19). And the UGF of performance of backup component $b_{i,j}$ in subsystem i, $u_{idle_{i,j}}(z)$ is calculated using Eq. (16). Then, if there is still performance deficiency in the subsystem i, it reallocates part of tasks to the idle backup component within the same subsystem.

$$\overline{\Delta}_i^h(z) = \Delta_i^h(z) \underrightarrow{\oplus} u_{idle_{i,j}}(z) \tag{26}$$

$$= \left(\sum_{b_i'=1}^{B_i'} \pi_{i,b_i'} z^{0, d_{i,b_i'}^h} + \sum_{b_i=1}^{B_i - B_i'} \pi_{i,b_i} z^{s_{i,b_i}^h, 0} \right) \underrightarrow{\oplus} \left(\sum_{b_{i,j}=1}^{B_{i,j}} \alpha_{i,b_{i,j}} z^{g_{i,b_{i,j}}^h} \right)$$

$$= \sum_{b_i'=1}^{B_i'} \sum_{b_{i,j}}^{B_{i,j}} \pi_{i,b_i'} \alpha_{i,b_{i,j}} z^{\max\left(g_{i,b_{i,j}}^h - d_{i,b_i'}^h, 0\right), \max\left(-g_{i,b_{i,j}}^h + d_{i,b_i'}^h, 0\right)} + \sum_{b_i=1}^{B_i - B_i'} \pi_{i,b_i} z^{s_{i,b_i}^h, 0}$$

$$= \sum_{\bar{b}_i=1}^{\overline{B}_i'} \overline{\pi}_{i,\bar{b}_i} z^{0, \bar{d}_{i,\bar{b}_i}^h} + \sum_{\bar{b}_i=1}^{\overline{B}_i - \overline{B}_i'} \overline{\pi}_{i,\bar{b}_i} z^{\bar{s}_{i,\bar{b}_i}^h, 0}$$

Where $\overline{B}_i'$ and $\overline{B}_i - \overline{B}_i'$ is the number of terms in the UGF that correspond to no performance surplus and no performance deficiency in subsystem i, respectively. $\overline{\pi}_{i,\bar{b}_i'}$ is the joint probability that the performance surplus is zero and performance deficiency is $\bar{d}_{i,\bar{b}_i'}^h$. $\overline{\pi}_{i,\bar{b}_i}$ is the joint probability that the performance surplus is $\bar{s}_{i,\bar{b}_i}^h$ and performance deficiency is zero.

Next, the UGF form of total performance surplus and total performance deficiency of subsystem i is calculated using Eq. (26) through iterative calculation.

$$\widetilde{\Delta}_i^h(z) = \Delta_i^h(z) \underrightarrow{\oplus} u_{idle_{i,1}}(z) \underrightarrow{\oplus} \cdots \underrightarrow{\oplus} u_{idle_{i,n}}(z) \tag{27}$$

$$= \left(\sum_{b_i'=1}^{B_i'} \pi_{i,b_i'} z^{0, d_{i,b_i'}^h} + \sum_{b_i=1}^{B_i - B_i'} \pi_{i,b_i} z^{s_{i,b_i}^h, 0} \right) \underrightarrow{\oplus} \left(\sum_{b_{i,1}=1}^{B_{i,1}} \alpha_{i,m_{i,1}} z^{g_{i,b_{i,1}}^h} \right)$$
$$\underrightarrow{\oplus} \left(\sum_{b_{i,2}=1}^{B_{i,2}} \alpha_{i,m_{i,2}} z^{g_{i,b_{i,2}}^h} \right) \underrightarrow{\oplus} \cdots \underrightarrow{\oplus} \left(\sum_{b_{i,n_b}=1}^{M_{i,n_b}} \alpha_{i,b_{i,n_b}} z^{g_{i,b_{i,n_b}}^h} \right)$$

$$= \left(\sum_{\bar{b}_i=1}^{\overline{B}_i'} \overline{\pi}_{i,\bar{b}_i} z^{0, \bar{d}_{i,\bar{b}_i}^h} + \sum_{\bar{b}_i=1}^{\overline{B}_i - \overline{B}_i'} \overline{\pi}_{i,\bar{b}_i} z^{\bar{s}_{i,\bar{b}_i}^h, 0} \right) \underrightarrow{\oplus} \left(\sum_{b_{i,2}=1}^{B_{i,2}} \alpha_{i,b_{i,2}} z^{g_{i,b_{i,2}}^h} \right) \underrightarrow{\oplus} \cdots \underrightarrow{\oplus} \left(\sum_{b_{i,n_b}=1}^{B_{i,n_b}} \alpha_{i,b_{i,n_b}} z^{g_{i,b_{i,n_b}}^h} \right)$$

$$= \sum_{\tilde{b}_i=1}^{\widetilde{B}_i'} \widetilde{\pi}_{i,\tilde{b}_i'} z^{0, \tilde{d}_{i,\tilde{b}_i'}^h} + \sum_{\tilde{b}_i=1}^{\widetilde{B}_i - \widetilde{B}_i'} \widetilde{\pi}_{i,\tilde{b}_i} z^{\tilde{s}_{i,\tilde{b}_i}^h, 0}$$

Where $\widetilde{B}_i'$ and $\widetilde{B}_i - \widetilde{B}_i'$ is the number of terms in UGF that correspond to no performance surplus and no performance deficiency in subsystem i, respectively. $\widetilde{\pi}_{i,\tilde{b}_i'}$ is the joint probability that the performance surplus is zero and performance deficiency is $\tilde{d}_{i,\tilde{b}_i'}^h$. $\widetilde{\pi}_{i,\tilde{b}_i}$ is the joint probability that the performance surplus is $\tilde{s}_{i,\tilde{b}_i}^h$ and performance deficiency is zero.

Subsequently, if there is still performance deficiency in the subsystem i, other subsystems with performance surplus transmit the performance surplus to it via the common bus. Therefore, Eqs. (21)-(24) is used to calculate the UGF of performance surplus, performance deficiency and performance storage under performance sharing during mission phase h.

$$\widetilde{U}_\Omega^h(z) = U_{\Omega 1}^h(z) \otimes_{\leftrightarrow} U_C(z) \otimes_{\leftrightarrow} \eta(z) \tag{28}$$

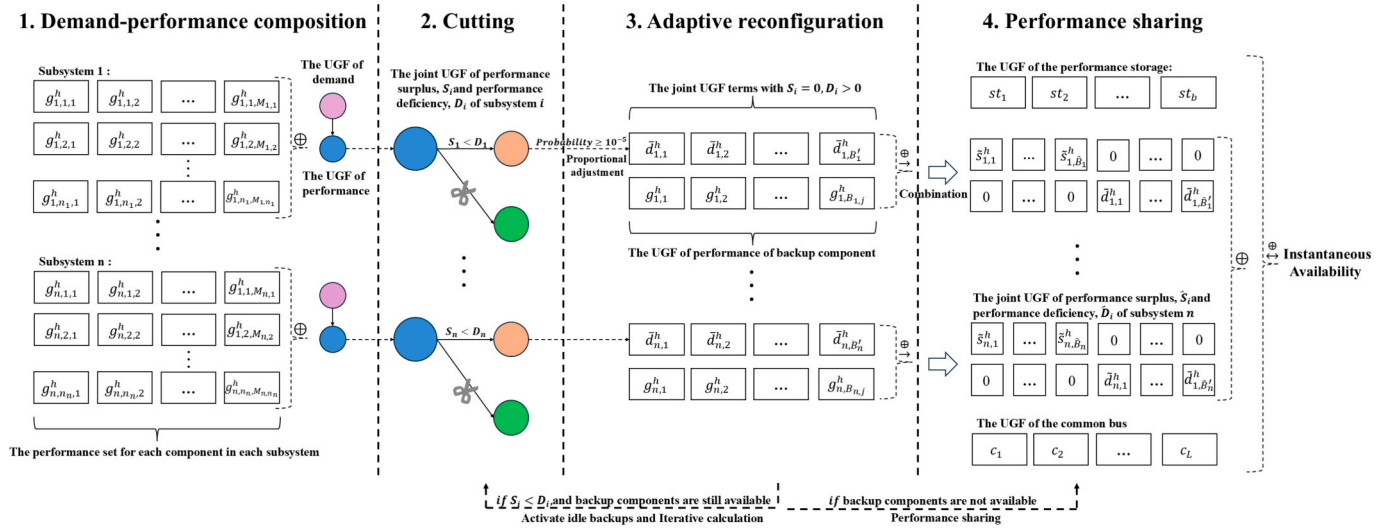

Fig. 5. The ucar algorithm.

$$= \sum_{j_b=1}^{J_B} pr_{j_b} z^{\tilde{s}_{j_b}^h, \tilde{d}_{j_b}^h, \tilde{U}_{j_b}^h}$$

Where $U_{\Omega 1}^h(z)$ is the UGF form of total performance surplus and total performance deficiency of system after adaptive reconfiguration. pr_{j_b} is the joint probability that the total performance surplus is $\tilde{s}_{j_b}^h$, the total performance deficiency is $\tilde{d}_{j_b}^h$, and the performance storage is $\tilde{U}_{j_b}^h$.

At last, according to Eq. (14) and Eq. (28), during phased mission h, the system instantaneous availability under the ABR mechanism is calculated by

$$A_1^h(t) = Pr\left(\tilde{d}_{j_b}^h = 0\right) \tag{29}$$

Based on Eq. (28), Eq. (29) and Table 2, the instantaneous availability under the ABR mechanism in the subsequent mission phases can be calculated using a similar approach. Additionally, to characterize the overall operation of the system, system availability can be obtained by time-averaging the instantaneous availability over the corresponding mission duration.

A PMS consist of two subsystem is illustrated to explain the solution process of the UGF technique, see Appendix A2.

4. Numerical example

In a small-scale power supply system, power plants convert thermal or wind energy into electricity using dedicated generators and transmit it to users to meet demand (Fig. 6). The power plant configures the number of its operational generators based on the probabilistic demand distribution within its designated region. The power plants are connected through a common bus. And, when a power plant experiences electricity shortage, other plants with higher generator output or lower demand can transmit the electricity surplus to the area with electricity deficiency via the common bus. If electricity surplus remains after performance sharing, it can be transmitted to a hydroelectric plant for storage.

During operation, generators are frequently affected by random disturbances such as degradation, strikes, and corrosion, which gradually reduce their output capacity. The RM mechanism and the ABR mechanism are employed to enhance system availability under disturbances. The RM mechanism involves periodic preventive maintenance on the operational generators. During maintenance, idle generators are activated to ensure a continuous power supply within the designated region.

The ABR mechanism is triggered when a power plant experiences electricity deficiency due to disturbances. The power plant sequentially activates its idle generators and reallocates part of power supply tasks to them. If the electricity deficiency persists after all idle generators have been activated, a portion of power supply task is further redistributed to the operational generators with electricity surplus in other power plants via the common bus.

In this context, the generator output can be regarded as the performance, while user electricity consumption is the demand. The structure and operational mechanism of a small-scale power supply system align with the proposed model. Therefore, the proposed modeling and assessment method is applicable for analyzing the trend of system instantaneous availability.

The investigated system comprises two thermal power plants, one wind power plant, and a hydroelectric plant. Each thermal power plant has four thermal generators (two backup generators), while the wind power plant consists of three wind generators (two backup generators). These power plants are connected via a common bus with capacity is $10 \times 10^8 kw/h$(Fig. 7). The technical specifications of each generator are detailed in Table 3. And, the state transition diagrams of thermal and

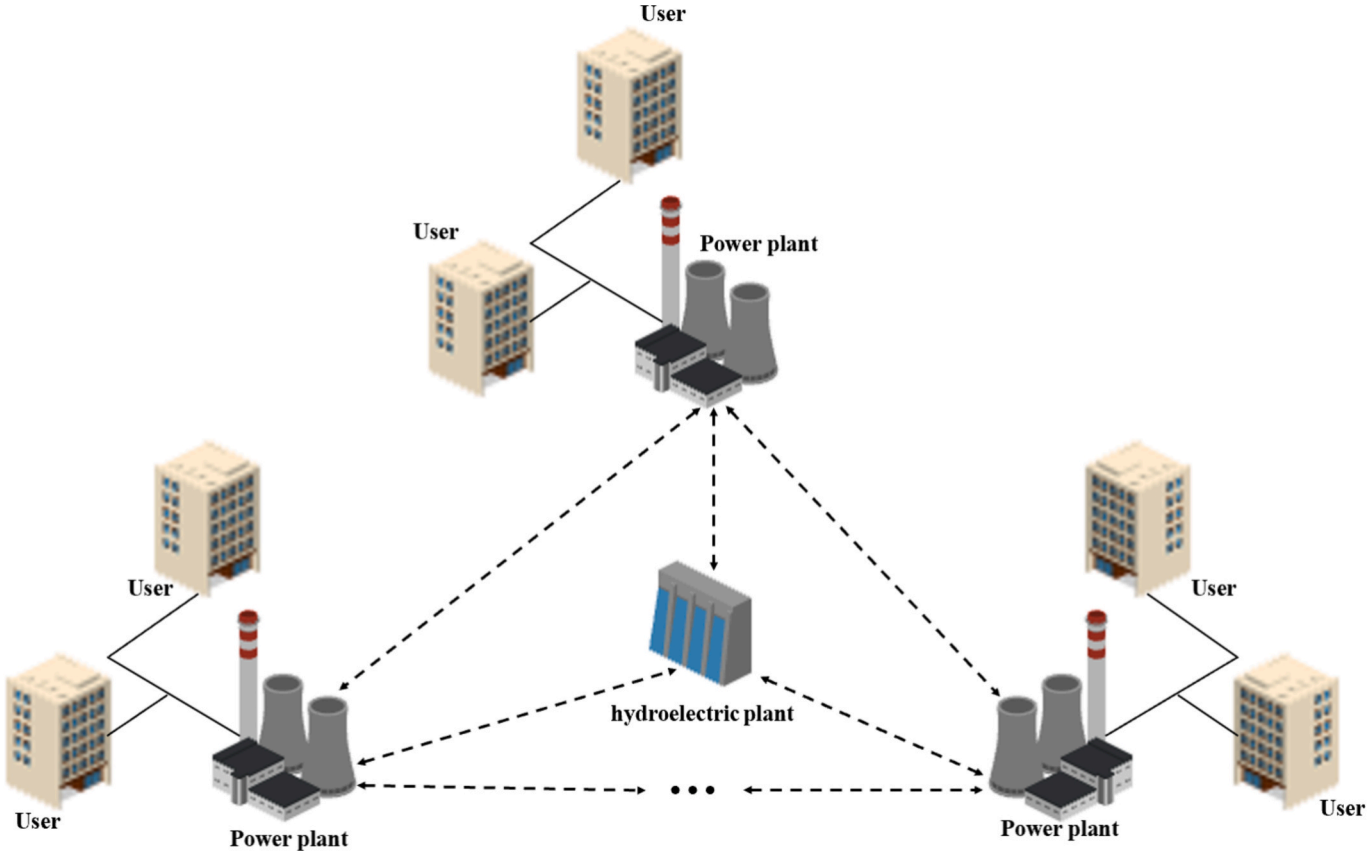

Fig. 6. Power distribution system.

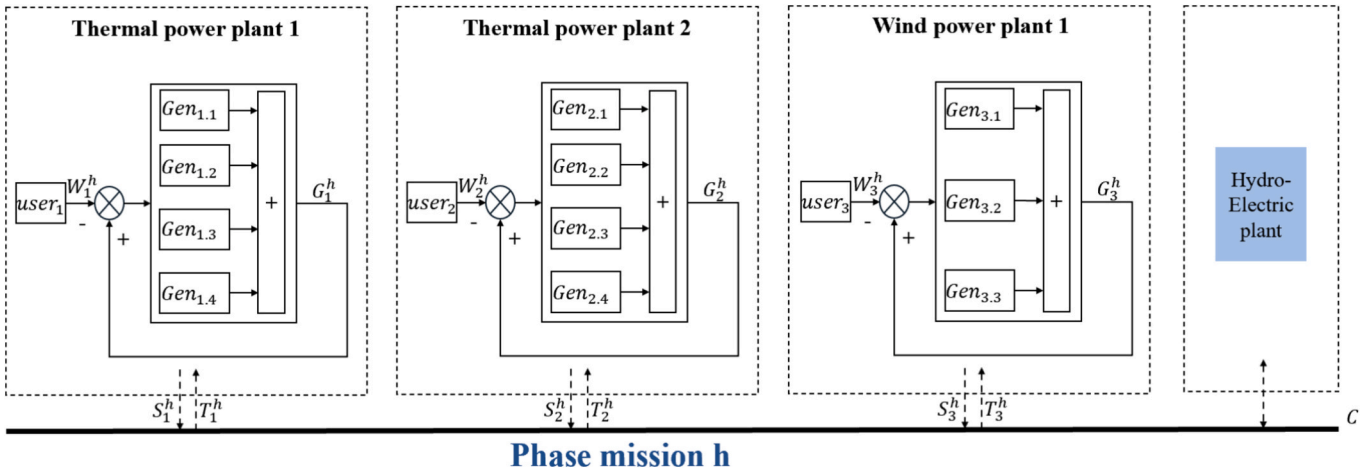

Fig. 7. The small-scale power supply system.

Table 3
The Performance and state transition rate of thermal and wind generators.

Generator	Performance Levels ($\times 10^8 kw/h$)	Performance state	Working state S_0	Slight damage state S_1	Serve damage state S_2	Fault state S_3	Initial state
Thermal	6	S_0	−0.0001	0.0001	0	0	1
	4	S_1	0	−0.0003	0.0003	0	0
	2	S_2	0	0.003	−0.0035	0.0005	0
	0	S_3	0.001	0	0.002	−0.003	0
Wind	5	S_0	−0.0001	0.0001	0	0	1
	3	S_1	0	−0.0002	0.0002	0	0
	1	S_2	0	0.004	−0.0044	0.0004	0
	0	S_3	0.002	0	0.003	−0.005	0

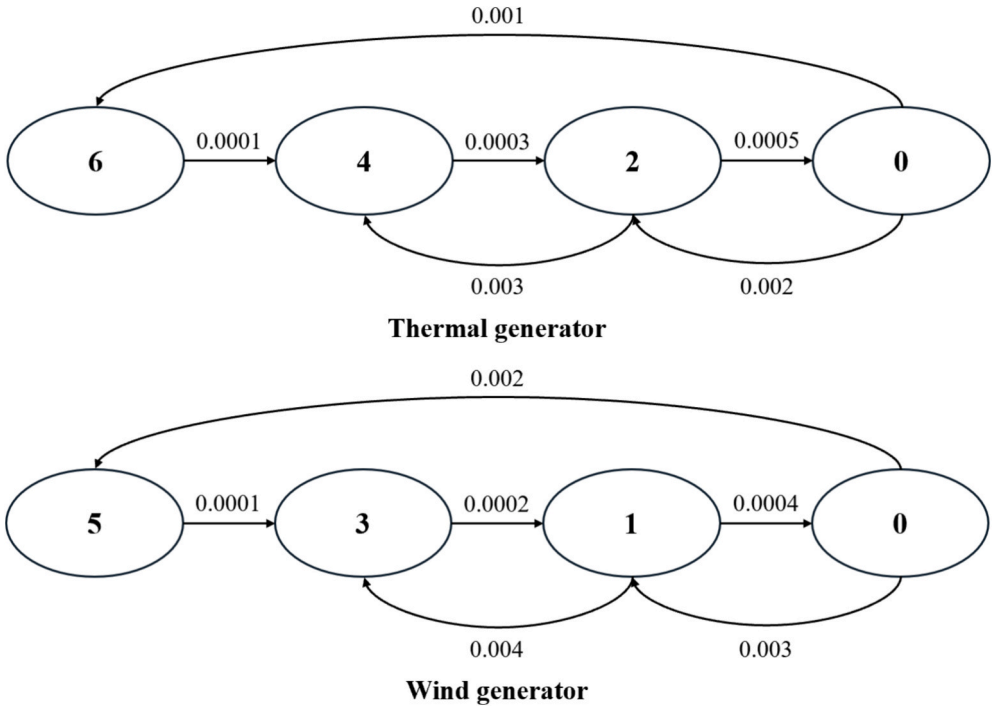

Fig. 8. The state transition of thermal and wind generators.

wind generators are shown as Fig. 8. The efficiency of the hydroelectric plant is 0.8. Moreover, we assume that hydroelectric plant can store all electricity surplus during operation.

Moreover, the system undergoes a phased mission process. The first phase involves a thermal power plant and corresponds to low-load phase. The second phase includes both a thermal power plant and a

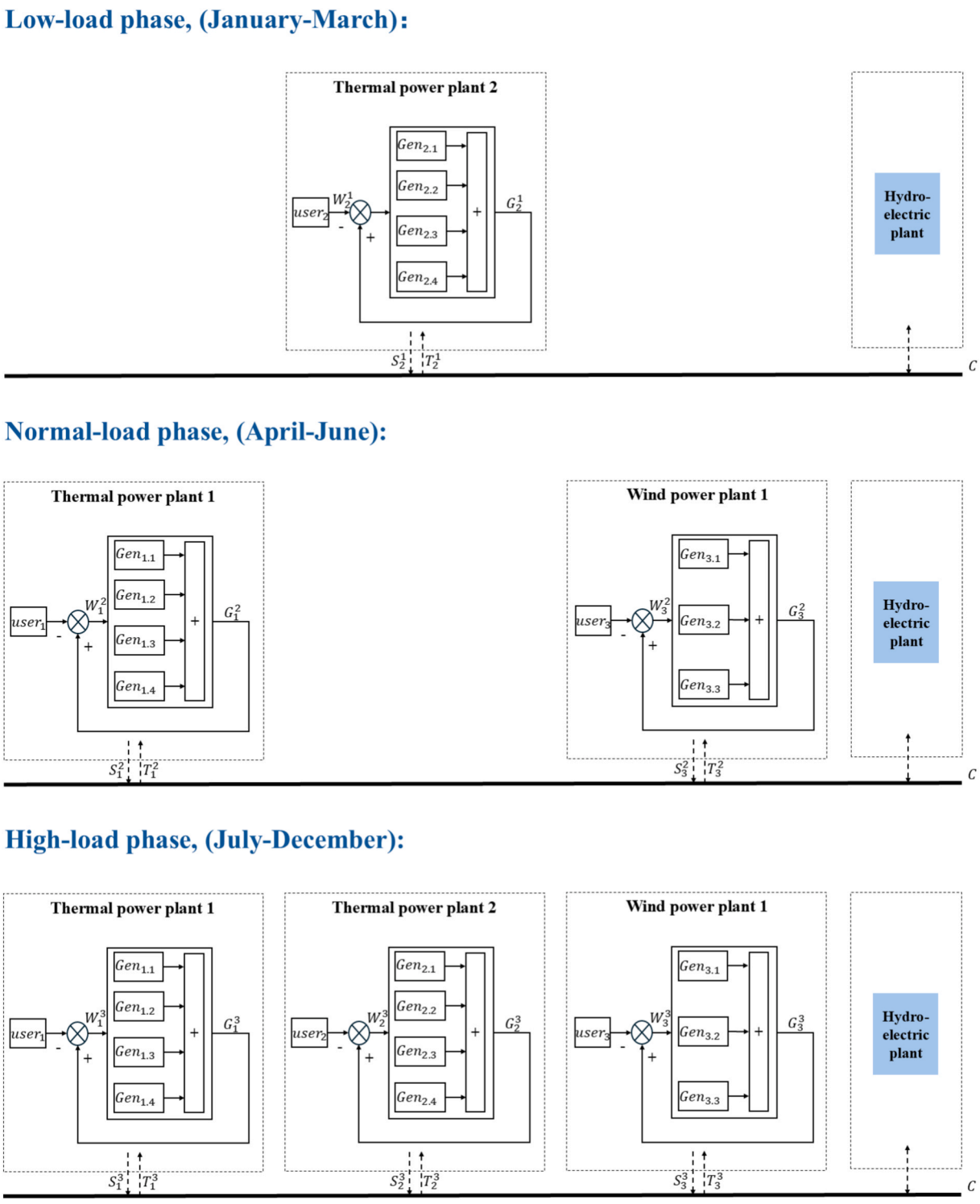

Fig. 9. A power supply system with phased missions.

Table 4
Demand distribution of each area.

Power plant	Demand ($\times 10^8 kw/h$)	Corresponding probabilities
Thermal power plant 1	[10,5]	[0.8,0.2]
Thermal power plant 2	[10,5]	[0.7,0.3]
Wind power plant 1	[5,0]	[0.7,0.3]

Table 5
The rotation period of power plants.

Power plant	Thermal 1	Thermal 2	Wind
Period	4	6	8

wind power plant, representing the normal-load phase. The third phase comprises two thermal power plants and a wind power plant, corresponding to the high-load phase (Fig. 9). The demand and its associated

Table 6
The intensity interval of random disturbances.

Disturbances intensity	Invalid disturbances	Normal disturbances	Extreme disturbances
Value interval	[0,9995]	(9995,9999)	(9999,10000)

probability for the designated region are provided in Table 4. Table 5 outlines the rotation cycle. Additionally, during the operation, the occurrence frequency of disturbances follows a Poisson process with an arrival rate of 1 (Tan et al., 2023). The intensity of disturbances follows a Uniform distribution $U(0, 10000)$, as detailed in Table 6. Invalid disturbances do not affect the generators. Normal disturbances can cause generators to transition from the working state S_0 to the severe damage state S_2, or from the slight damage state S_1 to the fault state S_3. And, extreme disturbances cause generators to transition from the working state S_0 to the fault state S_3 (Dui et al., 2024).

(1) The trend of availability of system considering degradation

According to Table 5, the minimum common multiple of the rotation intervals of the three power plants is $lcm(4, 6, 8) = 24$ months. In contrast, the overall system follows a 33-month rotation interval, as each power plant operates for 9 months with a one-year cycle. Fig. 10 illustrates that during each mission phase, the system availability decreases over time due to degradation. At specific time points (8,10,12,19,23,25, and 30), the RM mechanism is performed, resulting in a temporary increase in availability. Subsequently, as degradation continues, system availability declines again. Compared with system availability without RM mechanism, the rotational RM mechanism effectively enhances system availability under degradation. Moreover, during each mission phase, performance storage can mitigate the decline rate of system availability. When the RM mechanism is not considered, the rate of stored performance consumption increases as result of component degradation, while the amount of stored performance progressively decreases. Consequently, the effectiveness of performance storage (PS) in improving system availability gradually diminishes over time. For instance, during the time interval [31,33], the system availability with PS decreases from 0.1285 to 0.1073, and the system availability without PS under RM decreases from 0.1246 to 0.1047.

(2) The trend of availability of system considering degradation and external disturbances.

Fig. 11 indicates that compared with the RM mechanism, the ABR mechanism is a more effective way to improve system availability under both degradation and external disturbances. According to the tendency illustrated in Fig. 11A, the system availability under the ABR mechanism exhibits a fluctuating trend, initially decreasing before subsequently increasing. In contrast, the system availability under the RM mechanism deceases overtime. It displays a temporary improvement after each implementation of the RM mechanism before continuing its subsequent decreasing trend. Moreover, according to the results in Fig. 11A and Fig. 11B, in contrast to the RM mechanism, the impact of performance storage is more significant under the ABR mechanism. Due to the stored performance, the system availability demonstrates a short-term increasing trend in high-load phase.

(3) Sensitivity analysis.

In a small-scale power supply system, various factors influence the system instantaneous availability under disturbances. To examine the validity of the proposed method, a sensitivity is conducted under varying key parameters. This section analyzes the impact of three key factors on system instantaneous availability: the capacity of the common bus, the storage efficiency under the RM mechanism, and the number of backup components under the ABR mechanism.

For the RM mechanism under component degradation, Fig. 12A illustrates that when storage efficiency remains constant, increasing the capacity of the common bus enhances system availability. However, as the capacity of the common bus continues to increase, the marginal improvement in availability gradually diminishes. Additionally, as shown in Fig. 12B, when the capacity of the common bus remains constant, system availability increases as storage efficiency improves.

For the ABR mechanism under both component degradation and external disturbances, Fig. 13A illustrates that when the number of backup generators in both thermal power plants remains constant, the system availability increases with the number of backup generators in the wind power plant during normal-load and high-load phases. Similarly, as shown in Fig. 13B, when the number of backup generators in thermal power plant 2 and the wind power plant remains constant, increasing the number of backup generators in thermal power plant 1 leads to an improvement in system availability during normal-load and high-load phases. Moreover, the results indicate that increasing the number of thermal generators in thermal power plant 1 is more effective in improving system availability than increasing the number of wind generators during normal-load and high-load phases.

(4) Result analysis.

To demonstrate the advantage and validity of the proposed method, a comparative analysis with existing models is conduced. As shown in Fig. 14A, the existing model assumes a fixed number of generators during each mission phase (Cheng et al., 2020), which leads to an overestimation of system availability. In contrast, the proposed model incorporates demand-driven adjustments based on probabilistic demand, resulting in a lower but more realistic availability assessment that better reflects actual system behavior. In practical engineering applications, the number of operating power plants is typically determined by probabilistic demand distributions, which is a key factor for accurately modeling system performance but is not considered in the existing model. Additionally, Fig. 14B illustrates the trend of expected performance surplus in each mission phase decreases over time, with the rate of decrease slowing down. The existing model shows a higher expected performance surplus, which reflects a tendency to allocate more resource than actually required. This discrepancy arises because the existing model overlooks probabilistic demand variations, leading to a less realistic representation of system behavior.

Meanwhile, in existing research, the redundancy mechanism has been widely adopted to improve system availability under similar conditions (Su et al., 2020). Fig. 15 illustrates the trend of system availability under different recovery strategies. Compared with the RM mechanism, both ABR mechanism and redundancy mechanism are more effective in improving the ability of mitigating internal and external disturbances. The system availability under the redundancy mechanism

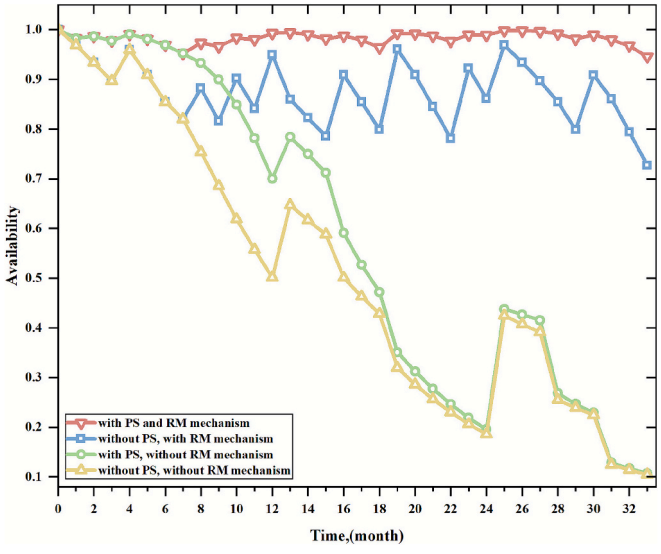

Fig. 10. Trend of system availability considering degradation

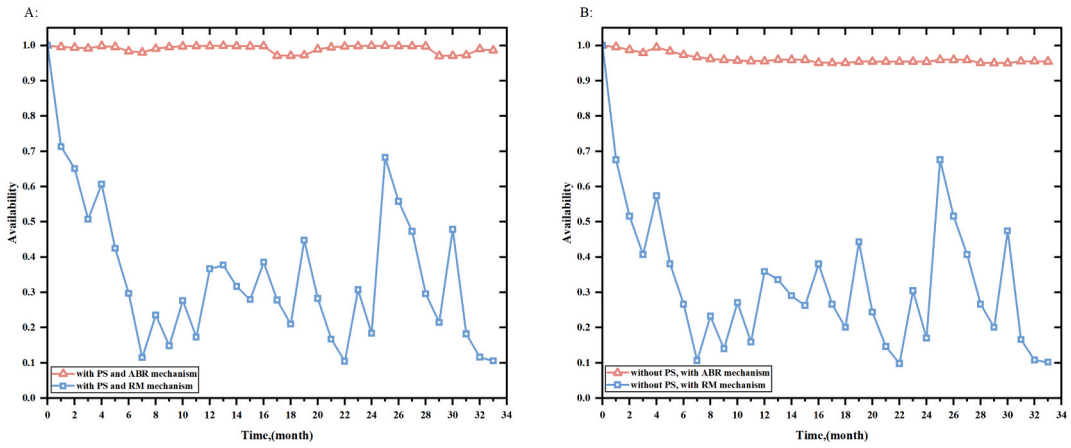

Fig. 11. Trend of system availability considering degradation and external disturbances.

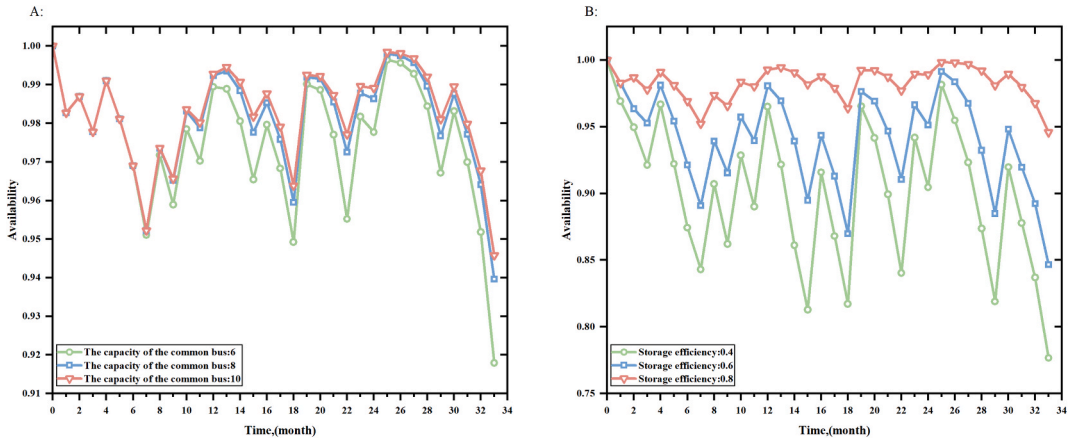

Fig. 12. The sensitivity of system availability under RM mechanism.

is slightly higher than that under the ABR mechanism. This is because the redundancy mechanism keeps all backup components continuously active, which enhances availability at the cost of increased resource consumption.

Meanwhile, we use expected performance surplus to represent the excessive electricity consumption. Accordingly, the cost of excessive consumption C_E is

$$C_E = C_{ele} \times E_{ps} \tag{30}$$

Where C_{ele} is the total cost of electricity production, E_{ps} is the expected performance surplus. According to reference (Nguyen et al., 2024), the total cost of electricity production is $0.0683 USD/kw.h$.

Then, we use efficiency-cost ratio to evaluate effectiveness of these recovery strategies. The efficiency-cost η_{EC} can be described as

$$\eta_{EC} = \frac{A^h(t)}{C_E + C_{ele} \times E_d} \tag{31}$$

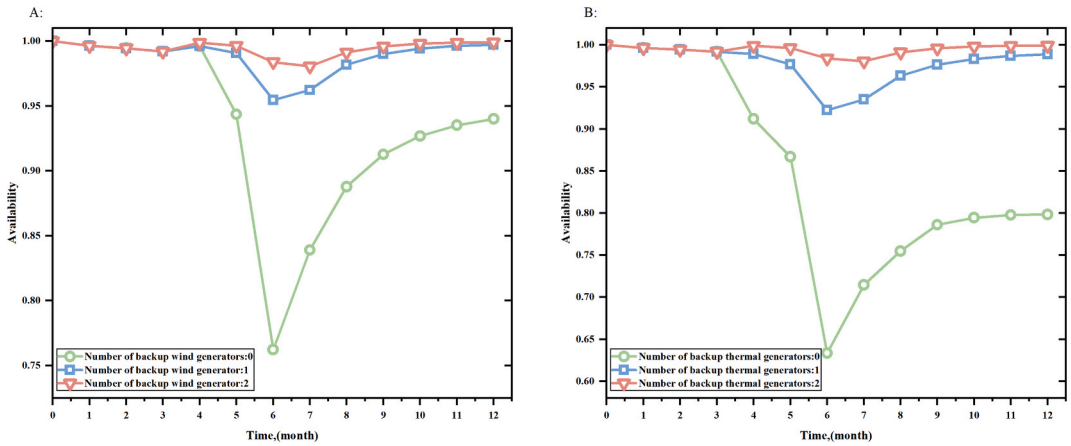

Fig. 13. The sensitivity of system availability under ABR mechanism.

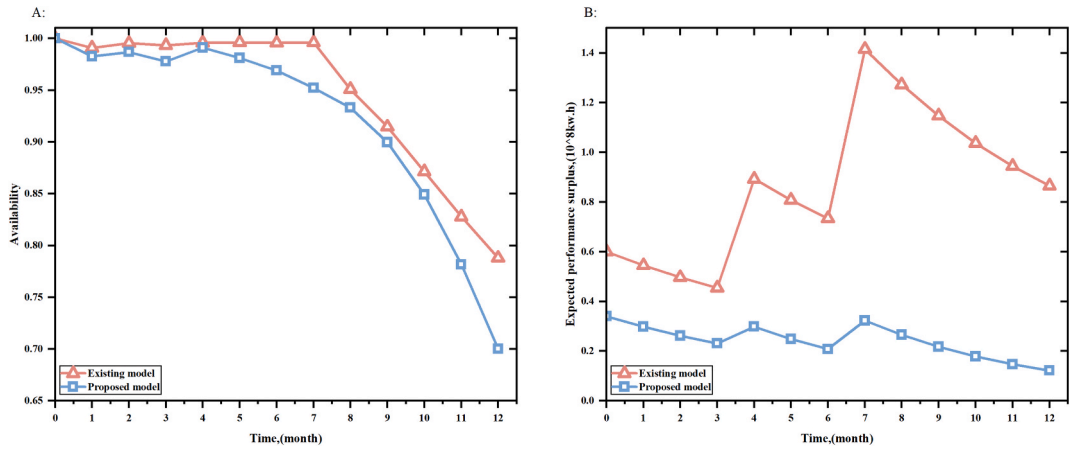

Fig. 14. Evaluation results obtained from different models.

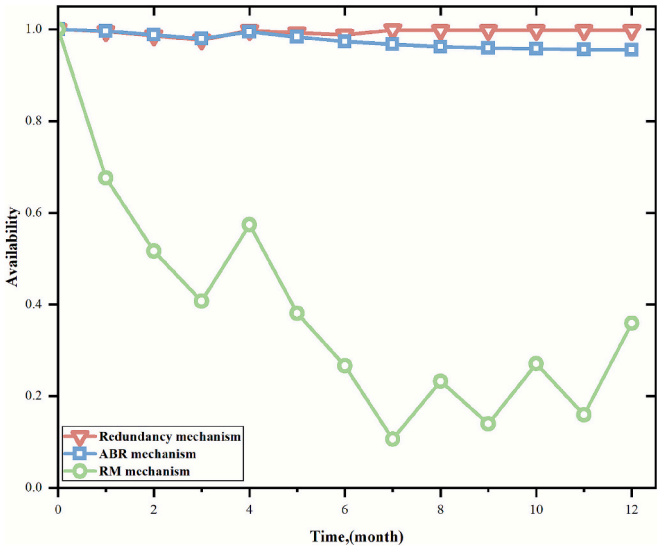

Fig. 15. The tendency of system availability under different recovery strategies.

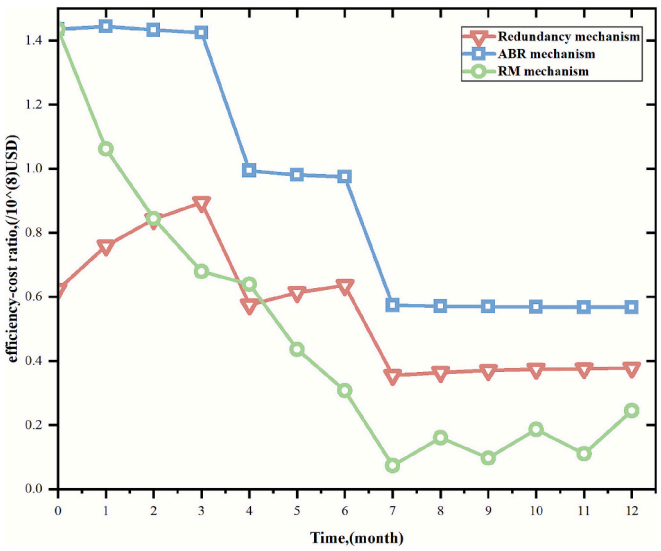

Fig. 16. The efficiency-cost ration of each recovery mechanism.

Where $A^h(t)$ is instantaneous availability of system at time t, E_d is the expected electricity demand.

Fig. 16 illustrates that the trend of efficiency-cost ratio during each mission phase. Compared with redundancy mechanism and RM mechanism, the efficiency-cost of ABR mechanism is higher. Therefore, the proposed ABR mechanism offers the advantage of enhancing the system's ability to withstand internal and external disturbances at lower cost.

In conclusion, compared with previous studies, the proposed model can evaluate instantaneous availability of a small-scale power supply system more accurately, as it accounts for the actual operation status. The proposed ABR mechanism is more effective in dealing with the external disturbances and degradation than the RM mechanism. This advantage arises because the RM mechanism operations on a predetermined preventive maintenance cycle and is limited in its ability to promptly address random disturbances due to its lack of real-time adaptability. Moreover, when only generator degradation is considered, the RM mechanism is more appropriate, as its scheduled maintenance effectively mitigates the internal disturbance and ensures the continuous operation of system. Therefore, in practical engineering applications, the ABR mechanism is preferable for responding to external disturbances, whereas the RM mechanism is more appropriate for managing predictable degradation.

5. Conclusion

This paper investigates the modeling and evaluation of a MS-PMS-CBPS, incorporating different recovery mechanisms under random disturbances. First, based on the existing models, we incorporate the impact of probabilistic demand on the operation state of the components and propose a demand-driven MS-PMS-CBPS considering performance storage. In contrast to existing studies, the proposed approach determines the number of operational components within each subsystem based on probabilistic demand distribution during each mission phase. Second, based on the proposed model, an ABR mechanism is developed to enhance system availability under disturbances. Then, we extend the model by integrating the combined effect of random disturbances and the ABR mechanism. Third, we develop the UGF-based instantaneous availability evaluation algorithm, enabling the assessment of instantaneous availability under the ABR mechanism. Finally, we use the proposed model and assessment method to analyze the instantaneous availability of a small-scale power supply system, validating the feasibility and providing a theoretical foundation for the design of small-scale power supply systems.

The results of the study indicate that the proposed model evaluates system instantaneous availability more accurately than existing models, as it does not rely on a fixed number of operational components predefined for each mission phase. Instead, it considers the probabilistic distribution of demand within each phase and configures the number of operational components accordingly. Additionally, the RM mechanism and the ABR mechanism is effective to enhance system instantaneous availability under disturbances. Meanwhile, the proposed ABR mechanism is more effective to deal with the disturbances than the RM mechanism. Moreover, although the ABR mechanism results in slightly lower system availability compared to the redundancy mechanism in existing studies, it offers significantly better cost-effectiveness, making it more practical and resource-efficient solution in real-world application.

However, several limitations still need to be addressed in future work. First, this study focuses on the rotational maintenance mechanism and the adaptive backup reconfiguration mechanism. Future research could explore additional recovery strategies to more effectively address disturbances. Second, external disturbances are modeling using existing approach. Developing a novel disturbance model is a key direction for future work.

CRediT authorship contribution statement

Gengshuo Hu: Methodology, Software, Validation, Writing – original draft. **Xing Pan:** Writing – review & editing, Methodology, Conceptualization, Supervision. **Linchao Yang:** Validation, Writing – review & editing.

Declaration of competing interest

The authors declare that they have no known competing financial interests or personal relationships that could have appeared to influence the work reported in this paper.

Acknowledgment

This work is supported by the National Natural Science Foundation of China under Grants No. 72071011 and 72401097.

Appendix

A1. Example 1

We use two illustrative examples to explain the recovery mechanisms: the rotational maintenance (RM) mechanism and the adaptive backup reconfiguration (ABR) mechanism. Under the RM mechanism, two units are initially in operation. After predefined rotation interval T, the idle backup units are active and take over the tasks, while the previously active units undergo preventive maintenance to restore them to optimal condition. The illustrated example is shown in Fig. A 1.

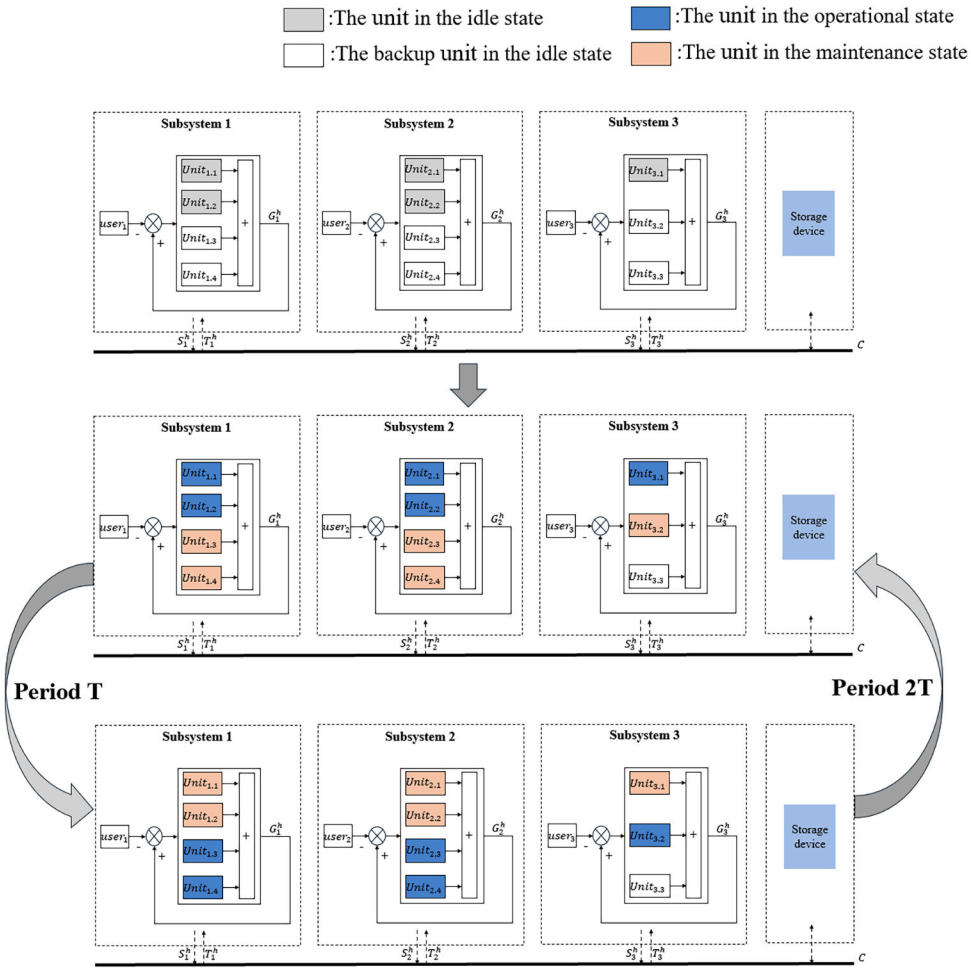

Fig. A1. Illustrated example of rotational maintenance mechanism.

Under the ABR mechanism, when subsystem 1 experiences a performance deficiency due to disturbances, its backup units are sequentially activated, and a portion of tasks is reallocated to these units. If performance deficiency still persists, part of the workload is further reallocated to the operational units in other subsystem via the common bus to ensure the system in the operation state. The illustrated example is shown in Fig. A 2.

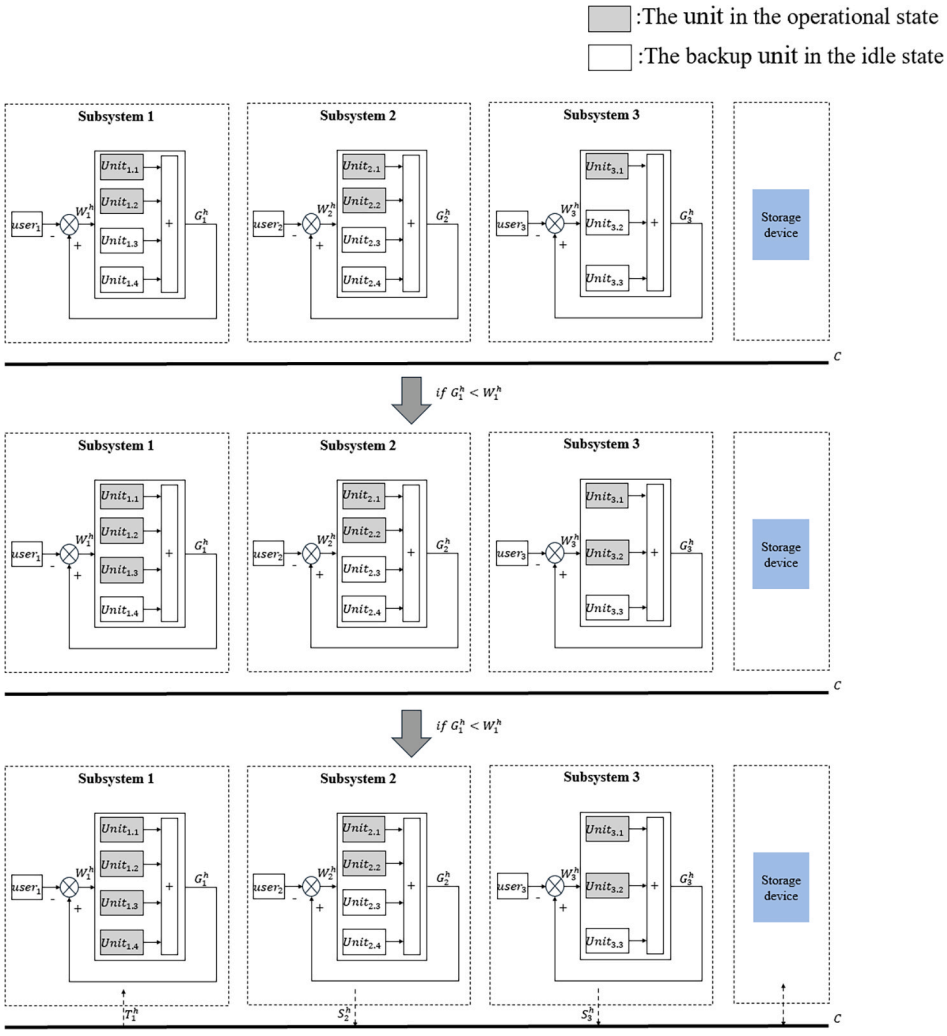

Fig. A2. Illustrated example of adaptive backup reconfiguration mechanism.

A2. Example 2

A small-scale power supply system that consists of a thermal power plant (two thermal generators and two backup thermal generators) and a wind power plant (one wind generators and two backup wind generators) is employed to illustrate the solution process of the UGF-based algorithms for system availability assessment. The corresponding parameters are detailed in Table A1, Table A2, and Table A3. For simplicity in this example, it is assumed that the generator performance levels and their associated probabilities remain unchanged as the system transitions from mission phase 1 at time t to mission phase 2 at time $t + \Delta t$.Moreover, the transmission capacity is $10 \times 10^8 kw/h$. The efficiency of the performance storage device is 0.8. We assume that performance storage device can store total performance surplus during the operation.

Table A1
Parameters of generators in Example at time t.

Generator	Performance level ($\times 10^8 kw/h$)	Corresponding probabilities
Thermal	[6,4,2,0]	[0.9,0.05,0.03,0.02]
Wind	[5,3,1,0]	[0.9,0.07,0.02,0.01]

Table A2
Parameters of area demands in Example (Phase 1).

Area	Power plant	Demand ($\times 10^8 kw/h$)	Corresponding probabilities
1	Thermal power plant 1	[10,5]	[0.4,0.6]
2	Wind power plant 1	[10,5]	[0.7,0.3]

Table A3
Parameters of area demands in Example (Phase 2).

Area	Power plant	Demand ($\times 10^8 kw/h$)	Corresponding probabilities
1	Thermal power plant 1	[15,10]	[0.8,0.2]

The following procedure is using proposed model and UGF algorithm to obtain system availability at time t_0.
(1) The UGF form of demand of each area is
Area 1:$\omega_1(z) = 0.4z^{10} + 0.6z^5$
Area 2:$\omega_2(z) = 0.7z^{10} + 0.3z^5$
(2) The UGF form of performance of each generator is
Thermal Generator:

$$u_{1j}(z) = 0.9z^6 + 0.005z^4 + 0.003z^2 + 0.002z^0$$

Wind Generator:

$$u_{2j}(z) = 0.9z^5 + 0.07z^3 + 0.02z^1 + 0.01z^0$$

(3) Based on the demand, the UGF form of plant s' performance can be presented as
Area 1 (demand is $10 \times 10^8 kw/h$):

$$u^1_{1,d_1}(z) = u^h_{1,1}(z) \oplus u^h_{1,2}(z)$$

$$= 0.81z^{12} + 0.09z^{10} + 0.0565z^8 + 0.039z^6 + 0.0029z^4 + 0.0012z^2 + 0.0004z^0$$

Area 2 (demand is $5 \times 10^8 kw/h$):

$$u^1_{1,d_2}(z) = 0.9z^6 + 0.005z^4 + 0.003z^2 + 0.002z^0$$

Area 1 (demand is $10 \times 10^8 kw/h$):

$$u^1_{2,d_1}(z) = u^1_{2,1}(z) \oplus u^1_{2,2}(z)$$

$$= 0.81z^{10} + 0.126z^8 + 0.0409z^6 + 0.018z^5 + 0.0028z^4 + 0.0014z^3 + 0.0004z^2 + 0.0004z^1 + 0.0001z^0$$

Area 2 (demand is $5 \times 10^8 kw/h$):

$$u^1_{2,d_2} = 0.9z^5 + 0.07z^3 + 0.02z^1 + 0.001z^0$$

(4) The UGF of performance surplus S_i and deficiency D_i of each plant is.
Thermal power plant:

$$\Delta^1_1 = u^1_{1,d_1}(z) \otimes 0.4z^{10} + u^1_{1,d_2}(z) \otimes 0.6z^5$$

$$= 0.324z^{2,0} + 0.675z^{1,0} + 0.036z^{0,0} + 0.00016z^{0,10} + 0.00048z^{0,8} + 0.00116z^{0,6} + 0.0012z^{0,5} +$$

$$0.01568z^{0,4} + 0.0018z^{0,3} + 0.0226z^{0,2} + 0.003z^{0,1}$$

Wind power plant:

$$\Delta^1_2 = u^1_{2,d_1}(z) \otimes 0.7z^{10} + u^1_{2,d_2}(z) \otimes 0.3z^5$$

$$= 0.837z^{0,0} + 0.0903z^{0,2} + 0.02923z^{0,4} + 0.0129z^{0,5} + 0.00196z^{0,6} +$$

$$0.00098z^{0,7} + 0.00028z^{0,8} + 0.00028z^{0,9} + 0.00007z^{0,10}$$

(5) The UGF form of total performance and deficiency vector without performance sharing by using an iterative method.

$$U_0(z) = z^{0,0}$$

$$U_1^1(z) = U_0^1(z) \underset{+}{\oplus} \Delta_1^1$$

$$= 0.324z^{2,0} + 0.675z^{1,0} + 0.036z^{0,0} + 0.00016z^{0,10} + 0.00048z^{0,8} + 0.00116z^{0,6} + 0.0012z^{0,5} +$$

$$0.01568z^{0,4} + 0.0018z^{0,3} + 0.0226z^{0,2} + 0.003z^{0,1}$$

$$U_2^1(z) = U_2^1(z) \underset{+}{\oplus} \Delta_2^1$$

$$= 0.2712z^{2,0} + 0.0293z^{2,2} + 0.5650z^{1,0} + 0.0301z^{0,0} + 0.1044z^{N,F}$$

Where $z^{N,F}$ means the term where there is no performance surplus but performance deficiency exists.

(6) The UGF of performance deficiency vector after performance sharing is

$$\overline{U}_\Omega^1(z) = U_2^1(z) \otimes_\leftrightarrow \eta(z)$$

$$= 0.2712z^{2,0} + 0.5650z^{1,0} + 0.0594z^{0,0} + 0.1044z^{N,F}$$

(7) Using Eq. (24) can obtain system availability after performance sharing.

$$A_0^1(t) = Pr\left\{\overline{d}_{j_a,i}^1 = 0\right\} = 0.8956$$

(8) Similarly, the system availability under the adaptive backup reconfiguration mechanism (ABR) can be calculated by using Algorithm 2.

$$A_1^1(t) = Pr\left\{\widetilde{d}_{j_b,i}^1 = 0\right\} = 0.9961$$

(9) The UGF of storage that can be used in next phase can be written as

$$C_{storage}(z) = 0.1785z^{8,0} + 0.0003z^{\frac{18}{25},0} + 0.0008z^{\frac{16}{25},0} + 0.5252z^{\frac{14}{25},0} + 0.0045z^{\frac{9}{25},0} + 0.0063z^{4,0} + 0.0008z^{\frac{8}{25},0} + 0.0025z^{\frac{6}{25},0} + 0.2725z^{\frac{4}{25},0} + 0.0029z^{\frac{4}{5},0}$$

(10) Similarly, the system availability in mission phase 2 can be calculated in following steps:

Step1: obtain the UGF of performance surplus S_i and deficiency D_i.

$$\Delta_1^2 = u_{1,d_1}^2(z) \otimes 0.8z^{15} + u_{1,d_2}^2(z) \otimes 0.2z^{10}$$

Step2: obtain the UGF of total performance surplus and deficiency vector considering performance storage $C_{storage}$.

$$U_1^2(z) = \Delta_1^2 \underset{+}{\oplus} C_{storage}(z)$$

Step3: obtain the UGF of performance deficiency vector under performance sharing.

$$\overline{U}_\Omega^2 = U_1^2(z) \otimes_\leftrightarrow \eta(z)$$

Step4: calculate the system availability after performance sharing.

$$A_0^2(t + \Delta t) = Pr\{\sum_{i=1}^{n} \overline{d}_{j_a,i}^2 = 0\} = 0.8810$$

Step5: calculate the system availability under the ABR mechanism.

$$A_1^2(t + \Delta t) = Pr\{\sum_{i=1}^{n} \widetilde{d}_{j_b,i}^2 = 0\} = 0.9998$$

A3. Notation table

Notation			
n	The number of subsystems	$\widehat{S}_i^h(t)$	The performance surplus of subsystem i after backup components are activated
$C_{storage}$	The capacity of the storage device	$\widehat{D}_i^h(t)$	The performance deficiency of subsystem i after backup components are activated
η_s	Storage efficiency	$\widehat{T}^h(t)$	The reallocated performance at time t during mission phase h under ABR mechanism

(continued on next page)

(*continued*)

W_i^h	The demand of subsystem i at during mission phase h	$\widetilde{D}^h(t)$	The performance deficiency of system at time t during mission phase h under ABR mechanism
$G_{i,j,\max}^h$	The performance of component j in its working state	$\widetilde{AP}^h(t)$	The available stored performance at time t during mission phase h under ABR mechanism
n_i^h	The number of operational components during mission phase h	$\widetilde{UP}^h(t)$	The utilized stored performance at time t during mission phase h under ABR mechanism
$G_{i,j}^h(t)$	The performance of subsystem i at time t during mission phase h	$\widetilde{RP}^h(t)$	The remaining stored performance at time t during mission phase h under ABR mechanism
$S_i^h(t)$	The performance surplus of subsystem i at time t during mission phase h	$\widetilde{C}_{storage}^h(t)$	The stored performance at time t during mission phase h under ABR mechanism
$D_i^h(t)$	The performance deficiency of subsystem i at time t during mission phase h	$\widetilde{S}^h(t)$	The performance surplus of system at time t during mission phase h under ABR mechanism
$S^h(t)$	The performance surplus of system at time t during mission phase h	$A^h(t)$	The system instantaneous availability at time t during mission phase h under ABR mechanism
$D^h(t)$	The performance deficiency of system at time t during mission phase h	$\omega_i^h(t)$	The UGF of $W_i^h(t)$
$T^h(t)$	The allocated performance during mission phase h	$u_{i,j}^h(t)$	The UGF of $G_{i,j}^h(t)$
$C(t)$	The capacity of the common bus	$u_{i,p_i}^h(z)$	The UGF of performance of subsystem i when the demand is w_{i,p_i}^h
$V^{h-1}(t)$	The stored performance in the previous mission phase	$\Delta_{i,p_i}^h(z)$	The joint UGF of performance surplus and performance deficiency of subsystem i when the demand is w_{i,p_i}^h
$\overline{D}^h(t)$	The performance deficiency of system at time t during mission phase h after performance sharing	$\Delta_i^h(z)$	The joint UGF of performance surplus and performance deficiency of subsystem i under different demand
$AP^h(t)$	The available stored performance at time during mission phase h under performance sharing	$U_\Omega^h(z)$	The joint UGF of joint pmf of $S^h(t)$ and $D^h(t)$
$UP^h(t)$	The utilized stored performance at time during mission phase h under performance sharing	$\eta(z)$	The UGF of $C(t)$
$\overline{RP}^h(t)$	The remaining stored performance at time during mission phase h under performance sharing	$U_c^h(z)$	The UGF of stored performance with no stored performance in device
$\overline{C}_{storage}^h(t)$	The performance storage at time t during mission phase h after performance sharing	$\overline{U}_\Omega^h(z)$	The joint UGF of performance surplus, performance deficiency and performance storage during mission phase h
$\overline{S}^h(t)$	The performance surplus of system at time t during mission phase h after performance sharing	$\widetilde{\Delta}_i^h(z)$	The joint UGF of performance surplus and performance deficiency when available backup components have been activated
$A_0^h(t)$	The system instantaneous availability at time t during mission phase h after performance sharing	$\widetilde{U}_\Omega^h(z)$	The joint UGF of performance surplus, performance deficiency and performance storage under ABR mechanism during mission phase h

Data availability

No data was used for the research described in the article.

References

Alhozaimy, S., Menascé, D. A., & Albanese, M. (2024). Resilience and performance quantification of dynamic reconfiguration. *Future Generation Computer Systems, 160*, 120–130. https://doi.org/10.1016/j.future.2024.05.040

Azhdari, A., & Ardakan, M. A. (2022). Reliability optimization of multi-state networks in a star configuration with bi-level performance sharing mechanism and transmission losses. *Reliability Engineering & System Safety, 226*, Article 108556. https://doi.org/10.1016/j.ress.2022.108556

Azhdari, A., Ardakan, M. A., & Najafi, M. (2023). An approach for reliability optimization of a multi-state centralized network. *Reliability Engineering & System Safety, 239*, Article 109481. https://doi.org/10.1016/j.ress.2023.109481

Bhatt, V., & Singh, S. B. (2025). Availability analysis of phase mission weighted components system with common bus performance sharing. *Reliability Engineering & System Safety, 260*, Article 111024. https://doi.org/10.1016/j.ress.2025.111024

Chen, G., Hu, Y., Wang, C., Wu, Z., Rong, W., & Guan, Q. (2025). Efficient reliability analysis of generalized k-out-of-n phased-mission systems. *Reliability Engineering & System Safety, 253*, Article 110581.

Cheng, C., Yang, J., & Li, L. (2020). Reliability assessment of multi-state phased mission systems with common bus performance sharing considering transmission loss and performance storage. *Reliability Engineering & System Safety, 199*, Article 106917. https://doi.org/10.1016/j.ress.2020.106917

Cheng, C., Yang, J., & Li, L. (2021a). Reliability assessment of multi-state phased mission systems with common bus performance sharing subjected to epistemic uncertainty. *IEEE Transactions on Reliability, 71*(3), 1281–1293.

Cheng, C., Yang, J., & Li, L. (2021b). Reliability evaluation of a k-out-of-n(G)-subsystem based multi-state phased mission system with common bus performance sharing subjected to common cause failures. *Reliability Engineering & System Safety, 216*, Article 108003. https://doi.org/10.1016/j.ress.2021.108003

Dui, H., Lu, Y., & Wu, S. (2024). Competing risks-based resilience approach for multi-state systems under multiple shocks. *Reliability Engineering & System Safety, 242*, Article 109773. https://doi.org/10.1016/j.ress.2023.109773

Gu, L., Wang, G., & Zhou, Y. (2024a). Optimal allocation of multi-state performance sharing systems with multiple common buses. *Reliability Engineering & System Safety, 247*, Article 110106. https://doi.org/10.1016/j.ress.2024.110106

Gu, L., Wang, G., & Zhou, Y. (2024b). Optimal resource allocation in common bus performance sharing systems with transmission loss. *Quality and Reliability Engineering International, 40*(7), 3675–3690. https://doi.org/10.1002/qre.3610

Gu, L., Wang, G., & Zhou, Y. (2025). Reliability analysis and optimization of multi-state tree-structured systems with performance sharing mechanism. *Reliability Engineering & System Safety, 260*, Article 110990. https://doi.org/10.1016/j.ress.2025.110990

Gu, L., Wang, G., & Zhou, Y. (2026). Reliability analysis of a complex series-parallel performance sharing system with performance excess failure and storage units. *Reliability Engineering & System Safety, 269*, Article 112070. https://doi.org/10.1016/j.ress.2025.112070

Gu, L., Wang, G., Zhou, Y., & Peng, R. (2024c). Reliability optimization of multi-state systems with two performance sharing groups. *Reliability Engineering & System Safety, 241*, Article 109580. https://doi.org/10.1016/j.ress.2023.109580

Gu, L., Wang, G., Zhou, Y., & Duan, F. (2025). Reliability Analysis of Ring-Structured Multistate Systems With Performance Sharing Mechanism Between Adjacent Units. *IEEE Transactions on Reliability, 1–14*. https://doi.org/10.1109/TR.2025.3637825

Hu, G., Pan, X., & Jiao, J. (2025). Resilience modeling and evaluation of multi-state system with common bus performance sharing under dynamic reconfiguration. *Reliability Engineering & System Safety, 260*, Article 111040. https://doi.org/10.1016/j.ress.2025.111040

Huang, D.-H., Chang, P.-C., & Lin, Y.-K. (2022). A multi-state network to evaluate network reliability with maximal and minimal capacity vectors by using recursive sum of disjoint products. *Expert Systems with Applications, 193*, Article 116421. https://doi.org/10.1016/j.eswa.2021.116421

Levitin, G. (2005). *The universal generating function in reliability analysis and optimization*. Springer.

Levitin, G. (2011). Reliability of multi-state systems with common bus performance sharing. *IIE Transactions, 43*(7), 518–524. https://doi.org/10.1080/0740817X.2010.523770

Levitin, G., Xing, L., & Huang, H. Z. (2019). Dynamic availability and performance deficiency of common bus systems with imperfectly repairable components. *Reliability Engineering & System Safety, 189*, 58–66. https://doi.org/10.1016/j.ress.2019.04.007

Levitin, G., Xing, L., & Xiang, Y. (2020). Series phased-mission systems with heterogeneous warm standby components. *Computers & Industrial Engineering, 145*, Article 106552. https://doi.org/10.1016/j.cie.2020.106552

Levitin, G., Xing, L., & Yu, S. (2014). Optimal connecting elements allocation in linear consecutively-connected systems with phased mission and common cause failures. *Reliability Engineering & System Safety, 130*, 85–94. https://doi.org/10.1016/j.ress.2014.04.028

Li, X.-Y., Li, Y.-F., Huang, H.-Z., & Zio, E. (2018). Reliability assessment of phased-mission systems under random shocks. *Reliability Engineering & System Safety, 180*, 352–361. https://doi.org/10.1016/j.ress.2018.08.002

Lin, C., Xiao, H., Xiang, Y., & Peng, R. (2023). Optimizing dynamic performance of phased-mission systems with a common bus and warm standby elements. *Reliability*

Engineering & System Safety, 240, Article 109598. https://doi.org/10.1016/j.ress.2023.109598

Lisnianski, A., & Ding, Y. (2009). Redundancy analysis for repairable multi-state system by using combined stochastic processes methods and universal generating function technique. *Reliability Engineering & System Safety, 94*(11), 1788–1795.

Nguyen, M. P., Ponomarenko, T., & Nguyen, N. (2024). Energy transition in vietnam: A strategic analysis and forecast. *Sustainability, 16*(5), 1969.

Peng, R. (2019). Optimal component allocation in a multi-state system with hierarchical performance sharing groups. *Journal of the Operational Research Society, 70*(4), 581–587. https://doi.org/10.1080/01605682.2018.1448697

Peng, R., Wu, D., Xiao, H., Xing, L., & Gao, K. (2019). Redundancy versus protection for a non-reparable phased-mission system subject to external impacts. *Reliability Engineering & System Safety, 191*, Article 106556. https://doi.org/10.1016/j.ress.2019.106556

Peng, R., Zhai, Q., & Yang, J. (2021). Reliability of Demand-Based Warm Standby System with Common Bus Performance Sharing. In *Reliability Modelling and Optimization of Warm Standby Systems* (pp. 123–143). Springer.

Rudek, R., & Rudek, I. (2024). Models and algorithms for the preventive maintenance optimization of railway vehicles. *Expert Systems with Applications, 240*, Article 122589. https://doi.org/10.1016/j.eswa.2023.122589

Sharifi, M., & Taghipour, S. (2022). Redundancy allocation problem of a Multi-State system with Binary-State continuous performance level components. *Expert Systems with Applications, 200*, Article 117161. https://doi.org/10.1016/j.eswa.2022.117161

Su, P., Wang, G., & Duan, F. (2020). Reliability evaluation of a k-out-of-n(G)-subsystem based multi-state system with common bus performance sharing. *Reliability Engineering & System Safety, 198*, Article 106884. https://doi.org/10.1016/j.ress.2020.106884

Su, P., Wang, G., & Duan, F. (2021). Reliability analysis for k-out-of-(n+ 1): G star configuration multi-state systems with performance sharing. *Computers & Industrial Engineering, 152*, Article 106991.

Tan, Z., Wu, B., & Che, A. (2023). Resilience modeling for multi-state systems based on Markov processes. *Reliability Engineering & System Safety, 235*, Article 109207. https://doi.org/10.1016/j.ress.2023.109207

Tang, M., Xiahou, T., & Liu, Y. (2023). Mission performance analysis of phased-mission systems with cross-phase competing failures. *Reliability Engineering & System Safety, 234*, Article 109174. https://doi.org/10.1016/j.ress.2023.109174

Tian, T., Yang, J., Li, L., & Wang, N. (2023). Reliability assessment of performance-based balanced systems with rebalancing mechanisms. *Reliability Engineering & System Safety, 233*, Article 109133. https://doi.org/10.1016/j.ress.2023.109133

Wang, C., Xing, L., & Levitin, G. (2015). Probabilistic common cause failures in phased-mission systems. *Reliability Engineering & System Safety, 144*, 53–60. https://doi.org/10.1016/j.ress.2015.07.004

Wang, J., Zhao, Y., Ma, X., Xiao, H., Ma, Y., Peng, R., & Yang, L. (2025). A State-Age-Dependent Maintenance-Spare Control Strategy Under Inspection Error Compensation. *IEEE Transactions on Reliability, 1–15*. https://doi.org/10.1109/TR.2025.3607028

Wu, C., Pan, R., Zhao, X., & Cao, S. (2021). Reliability evaluation of consecutive-k-out-of-n: F systems with two performance sharing groups. *Computers & Industrial Engineering, 153*, Article 107092. https://doi.org/10.1016/j.cie.2020.107092

Wu, C., Pan, R., Zhao, X., & Wang, X. (2024). Designing preventive maintenance for multi-state systems with performance sharing. *Reliability Engineering & System Safety, 241*, Article 109661. https://doi.org/10.1016/j.ress.2023.109661

Wu, C., Zhao, X., Wang, S., & Song, Y. (2025). Reliability analysis of weighted k-out-of-n: G performance sharing systems with multiple transmission loss levels. *Reliability Engineering & System Safety, 257*, Article 110859. https://doi.org/10.1016/j.ress.2025.110859

Xiao, H., Zhang, Y., Xiang, Y., & Peng, R. (2020). Optimal design of a linear sliding window system with consideration of performance sharing. *Reliability Engineering & System Safety, 198*, Article 106900. https://doi.org/10.1016/j.ress.2020.106900

Xing, L. (2007). Reliability Evaluation of Phased-Mission Systems With Imperfect Fault Coverage and Common-Cause Failures. *IEEE Transactions on Reliability, 56*(1), 58–68. https://doi.org/10.1109/TR.2006.890900

Yi, K., Xiao, H., Kou, G., & Peng, R. (2019). Trade-off between maintenance and protection for multi-state performance sharing systems with transmission loss. *Computers & Industrial Engineering, 136*, 305–315. https://doi.org/10.1016/j.cie.2019.07.030

Yu, H., Wu, X., & Wu, X. (2021). A Combinatorial Modeling Method for Mission Reliability of Phased-Mission System With Phase Backups. *IEEE Transactions on Reliability, 70*(2), 590–601. https://doi.org/10.1109/TR.2020.3003073

Yu, H., Yang, J., Lin, J., & Zhao, Y. (2017). Reliability evaluation of non-repairable phased-mission common bus systems with common cause failures. *Computers & Industrial Engineering, 111*, 445–457. https://doi.org/10.1016/j.cie.2017.08.002

Zhang, T., Mo, Y., & Yang, L. (2025). Reliability analysis of a capacitated series-parallel multi-state system subject to performance sharing mechanism and transmission loss. *Reliability Engineering & System Safety, 263*, Article 111249. https://doi.org/10.1016/j.ress.2025.111249

Zhao, X., Han, H., Jiao, C., & Qiu, Q. (2024). Reliability modeling of k-out-of-n: F balanced systems with common bus performance sharing. *Reliability Engineering & System Safety, 248*, Article 110144.

Zhao, X., Wu, C., Wang, S., & Wang, X. (2018). Reliability analysis of multi-state k-out-of-n: G system with common bus performance sharing. *Computers & Industrial Engineering, 124*, 359–369. https://doi.org/10.1016/j.cie.2018.07.034